Molecular Psychiatry (2021) 26:6002–6022
https://doi.org/10.1038/s41380-020-00956-4

ARTICLE

C/EBPβ is a key transcription factor for *APOE* and preferentially mediates ApoE4 expression in Alzheimer's disease

Yiyuan Xia[1,2] · Zhi-hao Wang[2,3] · Jichun Zhang[2] · Xia Liu[2] · Shan Ping Yu[4] · Karen X. Ye[5] · Jian-Zhi Wang[1] · Keqiang Ye[2] · Xiao-Chuan Wang[1,6]

Received: 14 July 2020 / Revised: 27 October 2020 / Accepted: 6 November 2020 / Published online: 18 December 2020

Abstract

The apolipoprotein E ε4 (*APOE4*) allele is a major genetic risk factor for Alzheimer's disease (AD), and its protein product, ApoE4, exerts its deleterious effects mainly by influencing amyloid-β (Aβ) and Tau (neurofibrillary tangles, NFTs) deposition in the brain. However, the molecular mechanism dictating its expression during ageing and in AD remains incompletely clear. Here we show that C/EBPβ acts as a pivotal transcription factor for *APOE* and mediates its mRNA levels in an age-dependent manner. C/EBPβ binds the promoter of *APOE* and escalates its expression in the brain. Knockout of C/EBPβ in AD mouse models diminishes ApoE expression and Aβ pathologies, whereas overexpression of C/EBPβ accelerates AD pathologies, which can be attenuated by anti-ApoE monoclonal antibody or deletion of ApoE via its specific shRNA. Remarkably, C/EBPβ selectively promotes more ApoE4 expression versus ApoE3 in human neurons, correlating with higher activation of C/EBPβ in human AD brains with ApoE4/4 compared to ApoE3/3. Therefore, our data support that C/EBPβ is a crucial transcription factor for temporally regulating *APOE* gene expression, modulating ApoE4's role in AD pathogenesis.

Introduction

In humans, *APOE* gene exists as three polymorphic alleles (ε2, ε3, and ε4) [1]. These allelic forms of *APOE* correspond to variations in the coding sequence of the gene leading to amino acid substitutions (Cys and Arg) at positions 112 and 158 of the protein. *APOE4* is the strongest genetic risk factor for Alzheimer's disease (AD) [2, 3], as *APOE4* significantly increases the risk for both early onset AD and late-onset AD [4, 5]. AD is the most-common neurodegenerative disease. The prominent pathological hallmarks include the extracellular senile plaques that are predominantly composed of amyloid-β (Aβ) peptides and intraneuronal neurofibrillary tangles (NFT) that principally consist of hyperphosphorylated and truncated Tau. The ε4 allele frequency is about 15% in the general population but as high as 40% in AD patients [6]. In addition to increasing the prevalence of AD, the presence of the *APOE4* allele also lowers the age of onset for AD in a gene dose-dependent manner [6, 7]. Mechanistically, ApoE4 seems to increase risk of AD and cognitive decline through both Aβ-dependent and Aβ-independent pathways [8–10]. ApoE isoforms differentially regulate Aβ production, aggregation, and clearance. For instance, histological analyses of AD

These authors contributed equally: Yiyuan Xia, Zhi-hao Wang

Supplementary information The online version of this article (https://doi.org/10.1038/s41380-020-00956-4) contains supplementary material, which is available to authorized users.

✉ Keqiang Ye
kye@emory.edu

✉ Xiao-Chuan Wang
wxch@mails.tjmu.edu.cn

1 Department of Pathophysiology, Key Laboratory of Ministry of Education of Neurological Diseases, Tongji Medical College, Huazhong University of Science and Technology, Wuhan, China

2 Department of Pathology and Laboratory Medicine, Emory University School of Medicine, Atlanta, GA 30322, USA

3 Department of Neurology, Renmin Hospital of Wuhan University, Wuhan, 430060 Hubei, China

4 Department of Anesthesiology, Emory University School of Medicine, Atlanta, GA 30322, USA

5 Emory College of Arts and Sciences, Emory University, Atlanta, GA 30322, USA

6 Co-innovation Center of Neuroregeneration, Nantong University, Nantong, 226001 JiangSu, China

brains reveal that ApoE is co-deposited with Aβ in amyloid plaques [11], indicating a direct association between ApoE and Aβ in AD pathogenesis. Synthetic Aβ peptides bind to ApoE either secreted from cells [12] or purified from human CSF [13] and plasma [14]. Furthermore, ApoE is essential for Aβ deposition in APP transgenic amyloid model mice. When *Apoe* knockout (KO) mice are crossed with amyloid model PDAPP or Tg2576 mice, Aβ deposition in the form of amyloid plaques and cerebral amyloid angiopathy is dramatically reduced [15, 16]. Independently of Aβ, ApoE4 might be less efficient than ApoE3 and ApoE2 in delivering cholesterol and essential lipids for maintenance of synaptic integrity and plasticity [17]. ApoE mediates the transport and delivery of cholesterol and other lipids through cell-surface ApoE receptors [1, 18]. The human ApoE protein is a 299 amino acid glycoprotein and is expressed in several organs, with the highest expression in the liver followed by the brain. ApoE is produced in abundance in the brain and serves as the principal lipid transport vehicle in CSF [19]. In the brain, astrocytes, microglia, vascular smooth muscle cells, and choroid plexus constitutively express ApoE, whereas neurons predominantly synthesize ApoE under stress conditions [20]. ApoE functions as a ligand in receptor-mediated endocytosis of lipoprotein particles [21]. Cholesterol released from ApoE-containing lipoprotein particles is used to support synaptogenesis and the maintenance of synaptic connections [22].

C/EBPβ, a member of the CCAAT/enhancer binding protein (C/EBP) family of transcription factors of the basic-leucine zipper class, is implicated in various cellular events including cell energy metabolism, cell proliferation and differentiation [23, 24]. C/EBPβ also plays a critical role in inflammation [25]. Promoters of many pro-inflammatory genes contain putative C/EBPβ consensus sequences [26], and C/EBPβ levels are upregulated in response to pro-inflammatory stimuli in macrophages [27] and glial cells [28]. Upon lipopolysaccharides treatment, C/EBPβ is highly upregulated both in astrocytes and in microglia [29]. On the other hand, C/EBPβ participates in memory formation and synaptic plasticity in neurons, and regulates the pro-inflammatory activation in glial cells [30]. Both pro-inflammatory genes and neurotoxic effects of activated microglia are attenuated in C/EBPβ-null brain [31]. Interestingly, C/EBPβ deficiency provides neuroprotection following ischemic [32] or excitotoxic injuries [33]. Expression of C/EBPs is enhanced in AD patient brains [34, 35], where Aβ stimulates C/EBPβ and C/EBP δ activation in glia cells [36]. Recently, we reported that brain C/EBPβ expression is increased in an age-dependent manner. It acts as a crucial transcription factor that drives expression of asparagine endopeptidase (AEP, gene name: *LMGN*). Overexpression of C/EBPβ facilitates AD pathologies partially through elevating AEP expression [37], which acts as δ-secretase and simultaneously cleaves both APP and Tau at N585 and N368 residues, respectively, promoting Aβ production and Tau aggregation. Deletion of AEP from 5xFAD or Tau P301S mice greatly ameliorates senile plaques and NFT pathologies, rescuing cognitive deficits in both mouse models [38, 39].

In the current report, we provide compelling evidence that C/EBPβ plays a pivotal role in dictating *APOE* gene expression by functioning as a transcription factor under physiological and pathological conditions. Depletion of C/EBPβ robustly diminishes *Apoe* expression in the wild-type and AD mouse brains. Overexpression of C/EBPβ in young 3xTg AD mouse model considerably augments ApoE levels and facilitates various AD pathologies, resulting in cognitive dysfunctions. Notably, monoclonal anti-ApoE antibody treatment or deletion of *Apoe* gene in these mice greatly alleviates AD pathologies and rescues cognitive activities. Strikingly, C/EBPβ preferentially promotes higher ApoE4 mRNA expression in human neurons compared to ApoE3. C/EBPβ displays more potent effects in human AD brains with ApoE4/4 than ApoE3/3. Consequently, ApoE4 protein levels are more abundant in AD patient brains with ApoE4/4 versus ApoE3/3, which is linked with C/EBPβ-induced AEP hyperactivation [37], leading to more robust APP and Tau proteolytic cleavage.

Materials and methods

Animals

Wild-type C57BL/6J mice (Stock No. 000664), 5XFAD mice (Stock No. 006554), 3XTg mice (Stock No. 034830) were obtained from the Jackson Laboratory. The C/EBPβ KO mice on a C57BL/6J background were generated as reported [40]. The animals were assigned to different experimental groups based on the litter and gender in a way that every experimental group had similar number of siblings' males and females. Primary rat cortical neuron and glia were cultured as previously described. All rats were bought from the Jackson Laboratory. Animal care and handling were performed according to NIH animal care guidelines and the Declaration of Helsinki and Emory Medical School guidelines. The protocol was reviewed and approved by the Emory Institutional Animal Care and Use Committee.

Human samples and cells

Postmortem brain samples were dissected from frozen brains of AD cases and non-demented controls from the Emory Alzheimer's Disease Research Center (Table S1). All procedures performed in studies involving human

participants were in accordance with the ethical standards of the institutional and/or national research committee and with the 1964 Helsinki declaration and its later amendments or comparable ethical standards. AD was diagnosed according to the criteria of the Consortium to Establish a Registry for AD and the National Institute of Aging. Diagnoses were confirmed by the presence of amyloid plaques and NFT in formalin-fixed tissue. Informed consent was obtained from the subjects. The study was approved by the Biospecimen Committee. HEK293 cells (ATCC) were cultured in high-glucose DMEM added with 10% fetal bovine serum (FBS), penicillin (100 units/ml)–streptomycin (100 μg/ml) (all from Hyclone). SH-SY5Y cells (ATCC) were cultured in RPMI 1640 added with 10% FBS, penicillin (100 units/ml)–streptomycin (100 μg/ml) (all from Hyclone). Cells were incubated at 37 °C in a humidified atmosphere of 5% CO_2.

Transfection and infection of the cells

The overexpressing plasmids were purchased from Addgene. The siRNAs were bought from Santa Cruz. Lipofectamine 3000 (Invitrogen) was used for HEK293 and SH-SY5Y cells transfection. The overexpression lentivirus (pFCGW-GFP) was packaged in the viral vector core of Emory University. The shRNA expressing lentivirus for HSF-1, C/EBPα, C/EBPβ, and ApoE were ordered from OriGene Technologies, Inc. (Rockville, MD).

Differentiation of human iPSC-derived NSCs into neurons

The used human induced pluripotent stem cell (iPSC)-derived NSCs were obtained from two donors: ax0111 from AD patient with ApoE4/4 genotype, ax0112 from AD patient with ApoE3/3 genotype (Axol Bioscience, Cambridge, UK). Neuron differentiation from NSCs was accomplished by culturing on PLO/Laminin-coated plates in neuronal differentiation medium, which contains DMEM/F12 + Neurobasal Medium (1: 1), GDNF (20 ng/ml), supplemented with BDNF, B27, N2(20 ng/ml), IGF (10 ng/ml), NT3 (10 ng/ml), ascorbic acid (200 μM) (all from Stemcell Technologies), and dbcAMP (100 nM) (Sigma-Aldrich). 48 h later, neuronal culture medium was changed to remove unattached cells, and then medium was half changed every 3 days during in vitro maturation.

Antibodies and reagents

AEP antibody AF2199 was bought from R&D. AEP antibody (clone 6E3, 11b7) was present from Dr Colin Watts, University of Cambridge. β-actin antibody was purchased from Sigma. Antibodies of C/EBPβ (C-19, H-7), GFP come from Santa Cruz Biotechnology (Santa Cruz, CA, USA). C/EBPα, p-C/EBPβ, APP, and NeuN antibodies were bought from Cell Signaling Technology. ApoE antibody (AB947) was bought from Millipore, ApoE antibody (701241), AT8, AT100, tau5 were bought from Thermo Fisher, and Aβ antibody (4G8) was bought from Covance. Mouse and human $A\beta_{40}$ and $A\beta_{42}$, IL-1β, TNF-α, IL-6 ELISA kits were purchased from Invitrogen, recombinant AEP was purchased from Novoprotein. More information is in Table S2.

Immunization of mice

Three months old male 3XTg mice were intraperitoneally injected weekly for 14 weeks with anti-mouse IgG or anti-ApoE monoclonal antibody (HJ6.3, as a gift from Dr David M. Holtzman, Washington University School of Medicine) at 10 mg of antibody/kg of body-weight dose. The working stock of antibody was freshly prepared on the date of injection at 1 mg/ml concentration.

Stereotactic injection

Briefly, animals were anesthetized with isoflurane vaporizer to 2% and given 0.1-mg/kg buprenorphine subcutaneously for pain management. After checked the depth of anesthesia via toe-pinch. The mice heads were shaved and restrained in a stereotaxic frame (Stoeltling, Wood Dale, IL). Sterile erythromycin ophthalmic ointment (0.5%) was applied to the eyes to prevent dryness and damage to the cornea. After the surface disinfection with iodophor and 70% ethanol, a small incision was made and exposing the skull landmarks lambda and Bregma. Hydrogen peroxide was used to clean the connective tissue. A small hole drilled through the skull with a bone drill. The coordinates of hippocampal were mediolateral ±1.5 mm, anteroposterior −2.1 mm, dorsoventral 1.8 mm, injected with 1 μL of AAV or/and 3 μL of LV. After injections, the incision was sutured and applied surface disinfection. The mice were monitored 1, 2, 7, and 10 days post surgery.

Immunoprecipitation and western blotting

The tissues or cells were washed with ice-cold PBS and lysed in RIPA buffer (20-mM Tris-HCl, pH 7.5, 1-mM EDTA, 1-mM EGTA, 150-mM NaCl, 2.5 mM sodium pyrophosphate, 1% NP-40, 1% sodium deoxycholate, 1-mM Na_3VO_4, and 1-mM β-glycerophosphate) with protease inhibitor cocktail for 20 min on ice. The supernatant was collected by centrifuging at 14,000 rpm for 20 min at 4 °C. Then the protein extract was diluted to 5 mg/ml. After electrophoresis, the samples were incubated overnight at 4 °C with the recommended amount of antibody, followed by detection of immunoblotting.

Real-time PCR

RNAs from cells and tissues were isolated with Trizol. After reverse transcription with SuperScriptIII reverse transcriptase, Real-time PCR reactions were performed using the ABI 7500-Fast Real-Time PCR System, Gene-specific primers and TaqMan Universal Master Mix Kit were designed and bought from Taqman. All kits and reagents were purchased from Life Technologies. $2^{-\Delta\Delta Ct}$ method was used for the relative quantification of gene expression. For each data point, at least 2 duplicated wells were used.

Luciferase Assay

HEK293 cells were seeded in 12-well plates and transfected with ApoE luciferase reporter together with pRL-TK Renilla luciferase plasmid (Promega), treated with/without overexpressing plasmids or siRNA. Foty-eight hours later, the cells were harvested in passive lysis buffer and analyzed using a Dual-Luciferase Reporter Assay System (Promega) on a microplate reader. The experiments were performed in triplicate.

Electrophoretic mobility shift assay (EMSA)

Nuclear proteins of HEK293 were extracted by NE-PER Nuclear and Cytoplasmic Extraction Reagents (Life Technologies). Double-stranded oligonucleotide probe for ApoE promoter or its mutations were labeled with biotin. Unlabeled probes were used as cold competitors. EMSA assay was performed according to the manufacturer's protocol of the LightShift Chemiluminescent EMSA Kit (Life Technologies).

Chromatin immunoprecipitation (ChIP)

HEK293 cells were fixed with 1% formaldehyde for 10 min and crosslinking was quenched with 2-M glycine for 5 min. After nuclei isolation, the chromatin was sonicated using a Covaris S220 sonicator to obtain the desired DNA fragment size (~500 bp). The sonicated chromatin was pre-cleaned by two rounds of centrifugation with maximum speed at 4 °C. Five microliter of anti-C/EBPβ (C-19, Santa Cruz) or 5 µl of anti-IgG (ab133470, Abcam) was used to precipitate the chromatin fragments that contain DNA-protein crosslinking ChIP samples, which was collected with 50-µl Dynabeads protein A (Invitrogen, 10001D). The enrichment of specific DNA sequences was examined by PCR using primer pairs of the different species ApoE promoters. PCR assay also detected each input sample and internal reference β-actin.

mAPOE-1066 F GGTTCTCAGTGCCCCAGT,
mAPOE-424 R AGCCACAGTTTGAAACCAGTC,
rAPOE-1153 F CACCTATTTCCATTTAAGCCTCCAG,
rAPOE-130 R ACAAACATCTCCACAATAGAGCATC,
hApoE-313 F TTACATTCATCCAGGCACAGG,
hApoE-201 R ATACAGACACCCTCCTCCAT.

AEP activity assay

Cell lysates (20 µg) or tissue homogenates (20 µg) and 20-µM AEP substrate Z-Ala-Ala-Asn-AMC (Bachem) were incubated with 200-µl reaction buffer, which contained 60-mM Na_2HPO_4, 20-mM citric acid, 1-mM EDTA, 1-mM DTT, and 0.1% CHAPS, pH 5.5 at 37 °C. Then the AMC-released fluorescence by substrate cleavage was measured in a fluorescence plate reader in kinetic mode at 460 nm.

Aβ plaque histology

For immunohistochemical stainning of Aβ, combined with Thioflavin-S staining. Briefly, free-floating 30-µm brain sections were treated with 0.3% H_2O_2 at room temperature (RT) for 10 min. After that, sections were washed in PBS with 0.3% Triton X-100 for three times, then 1% BSA was used for blocking for 30 min, followed by overnight incubation with anti-Aβ antibody (1:500, Sigma-Aldrich) at 4 °C. The signal was developed using the Histostain-SP kit. After the preparation, the sections were washed in distilled water and stained for 5 min with 0.0125% Thioflavin-S in 50% ethanol. After washing, the sections were covered with a glass cover using mounting solution and took pictures under a fluorescence microscope. The plaque number and plaque area were analyzed using the ImageJ software (National Institutes of Health).

Immunofluorescence (IF)

Transfected/treated cells or mice brain slices or human tissues were fixed and incubated for 24–48 h at 4 °C with primary antibodies followed by 1 h at 37 °C with Alexa Fluor® 568- or Alexa Fluor® 488- or Alexa Fluor® 647-conjugated secondary antibodies (Invitrogen). DAPI (1 µg/ml) (Sigma) was used for the nuclei staining. Images were acquired through Confocal (Olympus FV1000). To quantify the fluorescent intensities, we split multicolor images into the single channels and converted the single-channel color images to 8-bit grayscale, then copied the image to create a binary image. Next, a region of interest around the object was drawn and highlighted. The background was subtracted with rolling ball to create a binary version of the image with only two pixels' intensities: black = 0 and white = 255. After setting measurements and the "Redirect to" line to the name of the copy of the image, the image fluorescent intensities on the binary image were analyzed.

Golgi staining

After perfusion, mice brains were fixed in 10% formalin for 24 h, then put in 3% potassium bichromate for 3 days and change the buffer every day in darkness. After these, the brains were transferred into 2% silver nitrate solution for 1 week in darkness, change half of the buffer every 3 days. Sections were cut at 50 mm by shock slicer, dehydrated through a discontinuous ethanol gradient: 50, 70, 90, and 100%, then cleared in xylene and coverslipped.

Electron microscopy

Mice were perfused with ice-cold 2% glutaraldehyde and 3% paraformaldehyde in PBS. Then hippocampal slices were postfixed in cold 1% OsO4 for 1 h. Ultrathin sections (90 nm) were stained with uranyl acetate and lead acetate and viewed at 100 kV in a JEOL 200CX electron microscope. Synapses were identified by the presence of synaptic vesicles and postsynaptic densities.

Electrophysiology

Mice were anaesthetized with isoflurane and decapitated. Separated brains were dropped in ice-cold artificial cerebrospinal fluid (a-CSF) containing 3-mM KCl, 124-mM NaCl, 6.0-mM $MgCl_2$, 2.0-mM $CaCl_2$, 1.25-mM NaH_2PO_4, 26-mM $NaHCO_3$, and 10-mM glucose. Acute hippocampal transversal slices of 400 μm were prepared on ice. After incubation at RT in a-CSF for 60 min, slices were placed in a recording chamber (RC-22C, Warner Instruments) and perfused with a-CSF (containing 1-mM $MgCl_2$) at RT. The field excitatory postsynaptic potentials (fEPSPs) were recorded in CA1 stratum radiatum by a glass microelectrode filled with a-CSF with resistance of 3–4 MΩ. A 0.1-MΩ tungsten monopolar electrode was used to stimulate the Schaffer collaterals. The stimulation output (Master-8; AMPI, Jerusalem) was controlled by the trigger function of an EPC9 amplifier (HEKA Elektronik, Lambrecht, Germany). Data were filtered at 3 kHz and digitized at sampling rates of 20 kHz using Pulse software (HEKA Elektronik). The stimulus intensity (0.1-ms duration, 10–30 μA) was set to evoke 40% of the maximum fEPSP and the test pulse was applied at a rate of 0.033 Hz. long-term potentiation (LTP) of fEPSPs was induced by three theta-burst stimulation at 100 Hz, repeated three times with a 200-ms interval. The magnitudes of LTP are expressed as the mean percentage of baseline fEPSP initial slope.

Morris water maze

The water maze is a round, water-filled tank (52 inches diameter), which was surrounded by extra-maze visual cues that kept at the same position during the whole training time. The platform was placed in the NW quadrant of the maze. Water was made with right amount of fat-free milk powder, filled to cover the platform by 1 cm at 22 °C. Each mouse was given 4 trials/day, maximum trial length was 60 s for 5 consecutive days with a 15-min intertrial interval. If mice did not reach the platform in time, they were manually guided to stay on platform for another 10 s. After 5 days of task acquisition, a probe trial was presented. The platform was removed and the percentage of time spent in the quadrant was measured over 60 s. MazeScan (Clever Sys) was used for analyzing all trials latency and swim speed.

Contextual fear conditioning

Mice were placed in a test chamber (7″ W, 7″ D 3 12″ H, Coulbourn) composed of Plexiglass with a metal shock grid floor. After wiped with 70% alcohol, allowed the mice to explore the enclosure for 3 min. Following with three conditioned stimulus (CS)–unconditioned stimulus (US) pairings (tone: 2000 Hz, 85 db, 20 s; foot shock: 0.5 mA, 2 s) with a 1-min intertrial interval. One minute following the last CS–US presentation, mice were removed from the chamber. 24 h later, the mice were presented with a context test, during which subjects were placed in the same chamber used during conditioning on day 1, no shocks were given during the context test. The amount of freezing was recorded. On day 3, a cue test was performed, during which subjects were exposed to the CS in a novel compartment. Animals were allowed to explore the novel context for 2 min, the 85-db tone was presented later. The freezing behavior in the 6 min was recorded via a camera and the software provided by Coulbourn.

Statistics

In vitro assays, the experiments were conducted by a blind individual, who did not know the sample information. The animal's information for in vivo assays was decoded after all samples were analyzed. Sample size was determined by Power and Precision (Biostat). All data are expressed as mean ± SEM and analyzed by SPSS 12.0 (IBM) and GraphPad Prism statistical software (GraphPad Software). The level of significance between two groups was assessed with unpaired t test with Welch's correction. When there are more than two groups, one-way ANOVA and Bonferroni's multiple comparison test were applied. The two-way ANOVA and Bonferroni's post hoc test compared the differences between groups that have been split on two independent factors. A value of $p < 0.05$ was considered to be statistically significant.

Results

C/EBPβ specifically mediates ApoE expression in primary neural cells and in 3xTg mice

Our previous study shows that C/EBPβ is positively correlated with aging and AD [37]. Moreover, APOE4 increases the risk of AD by driving earlier and more abundant amyloid pathology in the brains of APOE4 carriers. Analyzing a large cohort of AD/control cases [41], we found that C/EBPβ expression levels positively correlated with ApoE levels, though ApoE genotype showed no significant difference between control and AD (Supplementary Fig. 1A–D and Table S3). Separating the analyses according to APOE genotypes, we observed a higher correlation between C/EBPβ and APOE4, especially within the AD group (R values = 0.1102, $p = 0.0212$ in control, R values = 0.28, $p = 0.0239$ in AD group). However, when we separated the cases into non ApoE4 and ApoE4 genotypes, we found that in brains from ApoE4 patients, ApoE4 mRNA levels were significantly higher in AD brains than in those of controls, while non ApoE4 groups still keep no difference (Supplementary Fig. 1E, F). To investigate the potential transcription factors regulating *APOE* gene expression in the brain during ageing, we analyzed its promoter with "alibaba2" software and identified numerous consensus DNA motifs for the putative transcription factors. Based on the criteria of both brain expression and temporal escalation during ageing, the literature search yielded only a handful of candidates including HSF-1, SP-1, c-Jun, Oct-1, C/EBPα, and C/EBPβ (Fig. 1A). To test whether any of these potential transcription factors indeed mediates *APOE* expression, we depleted them with their specific siRNAs in SH-SY5Y neuronal cell line. Immunoblotting validated that ApoE protein level was substantially diminished, when C/EBPβ but not C/EBPα was selectively knocked down. As a positive control, the downstream target of C/EBPβ, AEP, was strongly suppressed when C/EBPβ was knocked down (Fig. 1B and Supplementary Fig. 2B). AEP enzymatic activities basically echoed C/EBPβ expression levels (Supplementary Fig. 2A). Quantitative RT-PCR (qRT-PCR) analysis showed that knockdown of C/EBPβ or C/EBP α significantly repressed *APOE* mRNA levels, with the former much stronger than the latter (Fig. 1C). To further explore whether C/EBPβ modulates ApoE expression in primary astrocytes, we prepared the primary glial cultures from E18 rats, and infected the isolated astrocytes (DIV 9) with lentivirus expressing C/EBPβ or its specific shRNA. C/EBPβ overexpression augmented both ApoE and AEP protein levels, whereas depletion of endogenous C/EBPβ robustly eradicated both of them in primary astrocytes (Fig. 1D and Supplementary Fig 2C). qRT-PCR showed *Apoe* mRNA concentrations tightly coupled with C/EBPβ levels (Fig. 1E). Moreover, we made the similar observations in primary neurons (DIV 7). C/EBPβ overexpression augmented both ApoE and AEP protein levels, whereas depletion of endogenous C/EBPβ robustly eradicated both of them in primary neurons (Supplementary Fig. 2D, E). Thus, C/EBPβ tightly mediates ApoE transcription and protein expression in both primary astrocytes and neurons.

To assess whether C/EBPβ selectively facilitates ApoE expression in the brain, we injected lentivirus expressing either C/EBPβ, C/EBPα, or HSF-1 into the hippocampus of 3xTg mice and examined any pathological effects using immunohistochemistry (IHC) and IF staining. C/EBPβ but neither C/EBPα nor HSF-1 transcription factor selectively triggered ApoE expression in the hippocampus of 3xTg mice (Fig. 1F, top panels). Consequently, Aβ plaques, Tau hyperphosphorylation and aggregation and Tau N368, a proteolytic truncate by AEP, were all highly increased in brains induced to overexpress C/EBPβ. In addition, NeuN, a neuronal biomarker, was also diminished in the C/EBPβ-expressed hippocampus (2nd-bottom panels), suggesting neuronal loss. Quantitative analysis demonstrated that C/EBPβ overexpression significantly augmented ApoE immune-reactivity and was associated with pronounced elevation of Aβ, pathological Tau phosphorylation (AT8, AT100) and Tau N368 signals. The amount of NeuN-expressed was greatly lessened in C/EBPβ-overexpressed hippocampus as compared to brains in which C/EBPα or HSF-1 were overexpressed (Fig. 1G). Among a panel of transcription factors, only C/EBPβ overexpression selectively escalated ApoE and AEP protein levels in mouse hippocampus (Supplementary Fig. 2F). qRT-PCR analysis confirmed this specificity. Again, AEP was selectively activated when C/EBPβ was overexpressed (Supplementary Fig. 2G, H). Hence, C/EBPβ selectively mediates ApoE expression in primary astrocytes and neurons and in AD mouse model.

C/EBPβ binds *APOE* promoter and acts as a transcription factor for *APOE*

To examine whether C/EBPβ acts as a transcription factor for *APOE* gene, we conducted an *APOE* promoter luciferase assay in the presence of C/EBPββ. Since the *APOE* promoter contains several putative C/EBP-binding motifs, we generated a series of truncates by systemically deleting the binding domains one by one. The mapping assay revealed that the −305–+93 fragment possessed only one C/EBP-binding motif and displayed the transcriptional activity comparable to the full-length promoter (Supplementary Fig. 3A), suggesting that this domain contains the major C/EBPβ binding site on the *APOE* promoter. To investigate this finding further, we transfected HEK293 cells with this luciferase construct, followed by depletion of endogenous C/EBPβ by its siRNA. As expected, knockdown of C/EBPβ

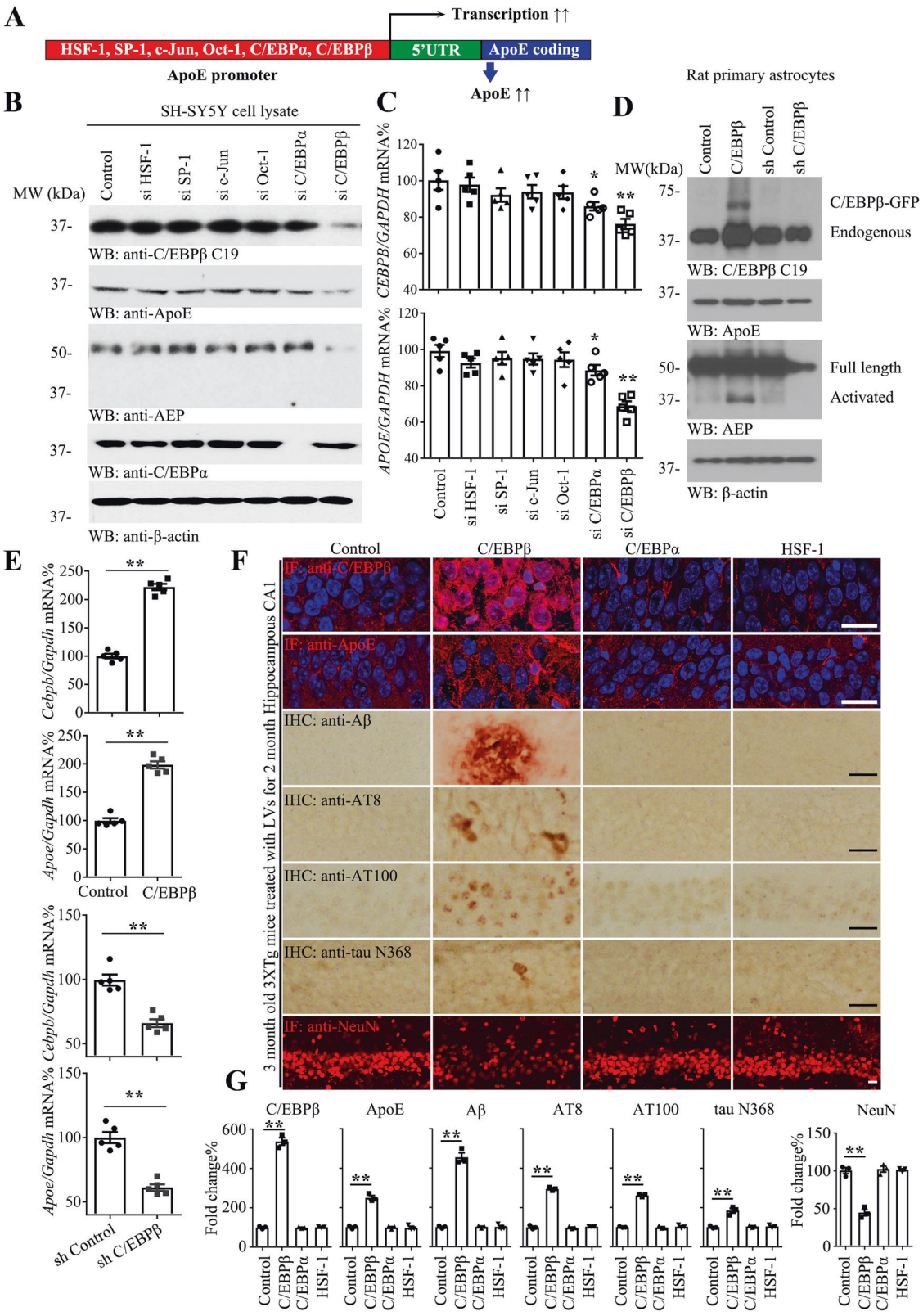

strongly mitigated the promoter luciferase activity (Supplementary Fig. 3B). On the other hand, overexpression of GFP-C/EBPβ greatly escalated luciferase activities, whereas a point mutation of the binding motif disabling C/EBPβ association (−305–+93 mut1) completely abolished the stimulatory effect. By contrast, a second mutation (mut2)

◀ **Fig. 1 C/EBPβ mediates the expression of ApoE in SH-SY5Y cells.** **A** Six putative ApoE transcription factors were predicted by "alibaba2" online program (http://gene-regulation.com/pub/programs/alibaba2/index.html). **B, C** SH-SY5Y cells were transfected with various siRNAs, and 48 h later, cells lysates were analyzed by western blot and mRNAs were analyzed by real-time PCR. (Mean ± SEM, $*P < 0.05$, $**P < 0.01$ vs. control, $n = 5$, two-way ANOVA and Bonferroni's post hoc test). **D, E** C/EBPβ mediates ApoE expression in primary astrocytes. Overexpression of C/EBPβ increased ApoE expression but knockdown of it reduced ApoE expression in vitro. Western blot and real-time PCR were conducted from primary astrocytes (DIV. 9 days) infected with virus overexpressing or shRNA against C/EBPβ for 7 days. (Mean ± SEM, $*P < 0.05$, $**P < 0.01$, $n = 5$, two-tailed student's t test). **F** Overexpression of C/EBPβ, C/EBPα, and HSF-1 in 3 months old 3XTg mice hippocampus by lentivirus for 2 months, then immunostaining of C/EBPβ, ApoE, Aβ, AT8, AT100, tau N368, and NeuN in hippocampal CA1, bar scales: 20 μm. **G** Quantification of ApoE, Aβ, AT8, AT100, tau N368, and NeuN immune-reactivities represented mean ± SEM, of 5–7 sections from three mice in each group ($**P < 0.01$, one-way ANOVA and Bonferroni's multiple comparison test). See also Supplementary Fig. 2.

failed to do so (Supplementary Fig. 3C). To further assess whether C/EBPβ interacts with the DNA sequence on the *APOE* promoter and mediates its transcription, we conducted an EMSA. C/EBPβ-containing nuclear extract potently bound to the hot probe, which was entirely stripped away by excessive cold probe or mut 1 probe; in contrast, mut 2 probe was unable to compete C/EBPβ from the hot probe, fitting with its robust luciferase activity in Supplementary Fig. 3C. Of note, anti-C/EBPβ but not control IgG elicited a super-shift on the gel, supporting that C/EBPβ specifically associated with the hot probe (Supplementary Fig. 3D). To ensure that C/EBPβ indeed interacts with the *APOE* promoter in the intact cells, we performed a standard ChIP assay, and discovered that C/EBPβ antibody but not control IgG selectively pulled down C/EBPβ bound to the *APOE* promoter, resided in the shredded genomic DNA. In addition, we also performed ChIP assays with mouse and rat brain tissues, which showed that C/EBPβ bound to the *Apoe* promoters from these species (Supplementary Fig. 3E), though the DNA sequences for the binding motifs on the promoters were different among the species. Therefore, C/EBPβ selectively binds to the *APOE* promoter and functions as its specific transcription factor.

C/EBPβ mediates Aβ-triggered ApoE expression

Neurons express ApoE under stressful conditions, especially under AD-related stress [20, 42]. To assess whether C/EBPβ modulates Aβ-induced ApoE, we treated neurons, astrocytes, and microglia with different concentrations of $Aβ_{42}$ oligomers for 24 h. Immunoblotting revealed that Aβ oligomers produced C/EBPβ upregulation in a dose-dependent manner, correlating with escalated ApoE and AEP levels. Notably, elevated AEP was proteolytically activated (Supplementary Figs. 4A, E and 5A). qRT-PCR confirmed that both *Cebpb* and *Apoe* mRNA levels were increased by $Aβ_{42}$ oligomers stimulation (Supplementary Figs. 4B, F and 5B). Knocking down C/EBPβ selectively attenuated both *Cebpb* and *Apoe* mRNA and protein expression levels triggered by $Aβ_{42}$ oligomers (Supplementary Figs. 4C, D, G, H and 5A, B). IF co-staining revealed that C/EBPβ and ApoE were detectable in GFAP-positive astrocytes, and expression of both was greatly escalated upon Aβ oligomers treatment. However, deletion of C/EBPβ substantially mitigated ApoE expression (Supplementary Fig. 4I), suggesting that C/EBPβ is mainly accountable for ApoE upregulation induced by $Aβ_{42}$ oligomers. To explore whether C/EBPβ mediates ApoE expression in AD mouse models, we injected AAV-GFP virus, AAV-GFP-C/EBPβ into the hippocampus of 3xTg mice (3 months old). Three months later, we found that the overexpression of C/EBPβ potently increased protein levels of both ApoE and AEP in wild-type and in 3xTg mice. On the other hand, deletion of endogenous C/EBPβ reduced both ApoE and AEP proteins as compared to vector (Supplementary Fig. 4J). qRT-PCR validated the relationship between C/EBPβ and *Apoe* mRNAs in mice (Supplementary Fig. 4K). Hence, C/EBPβ mediates *Apoe* expression in various cell types including neurons, astrocytes, and microglia. Moreover, it also regulates *Apoe* transcription and protein expression in AD mouse models.

To further explore whether C/EBPβ mediates ApoE expression in neurons, we employed our newly developed Thy1-C/EBPβ transgenic mice that primarily overexpress human C/EBPβ in neurons. Noticeably, neuronal C/EBPβ strongly escalated ApoE mRNA and protein levels in an age-dependent manner (Supplementary Fig. 5C, D). IF co-staining demonstrated that ApoE was greatly elevated in both NeuN, GFAP, and Iba-1-positive cells in Thy1-C/EBPβ transgenic mouse brains in an age-dependent way as compared to wild-type littermates (Supplementary Fig. 6A–C). Quantification of ApoE signals in these cells is summarized in Supplementary Fig. 6D. We also conducted IF co-staining on human brain sections and found that C/EBPβ was much more highly expressed in NeuN or GFAP-positive cells in AD brains than in sections from control brains. Though both Iba-1 and C/EBPβ expression levels were clearly elevated in AD brains compared to controls, C/EBPβ IF did not co-localize with Iba-1 signals (Supplementary Fig. 7), indicating that elevated C/EBPβ might mainly be distributed in neurons and astrocytes but not microglia. Hence, C/EBPβ mediates endogenous mouse ApoE expression. They both co-distribute in neurons and astrocytes in human AD brains.

C/EBPβ regulates ApoE expression in an age-dependent manner

Ageing is the major risk factor for AD pathologies. To test whether C/EBPβ regulates ApoE expression temporally, we monitored its mRNA and protein levels in the brains from different ages of wild-type mice. Consistent with our previous findings [37], expression of both C/EBPβ and its downstream target AEP gradually increased in an age-dependent way, with AEP proteolytic activation observed in 180- and 360-day old mouse brains. *Apoe* mRNA and protein concentrations were augmented in the same temporal format (Fig. 2A). KO of C/EBPβ substantially abolished both ApoE and AEP protein expression. Again, qRT-PCR showed that *Apoe* mRNA levels were significantly decreased in C/EBPβ-null mice brains (Fig. 2B). IF co-staining revealed that C/EBPβ and ApoE were detectable in NeuN-positive hippocampal neurons on wild-type mouse brain sections. In contrast, they were barely demonstrable in C/EBPβ+/− littermates (Fig. 2C).

Next, we extended our study into human AD patient samples. *APOE* mRNA concentrations were age-dependently increased in controls. Notably, human AD brains exhibited significantly more abundant *APOE* mRNA than age-matched controls. AEP enzymatic activities also revealed a similar pattern (Fig. 2D, top and middle panels). Immunoblotting indicated that both C/EBPβ and ApoE levels progressively increased in the brains with age in the healthy controls. In brains from AD patients, higher levels of both proteins were found than in healthy controls. The positive control, AEP, was not only upregulated with age but is also proteolytically active in AD patients (Fig. 2D, bottom panels), consistent with our previous findings [38, 39]. IF co-staining showed that both C/EBPβ and ApoE were increased in human AD brains versus healthy controls. Noticeably, C/EBPβ mainly resided in the cytoplasm in the control brains, but it predominantly distributed in the nuclei of AD brains (Fig. 2E). Thus, C/EBPβ mediates ApoE expression age-dependently and stimulates its levels in AD brains.

C/EBPβ mediates the expression of ApoE in AD mouse models

To explore whether C/EBPβ is required for ApoE expression in AD mouse models, we determined their protein levels in 3xTg/C/EBPβ+/+, 3xTg/C/EBPβ+/−, and 3xTg/C/EBPβ−/− mice, and compared them with age-matched C/EBPβ+/+, C/EBPβ+/−, and C/EBPβ−/− mice. In addition, we also deleted C/EBPβ from 5xFAD mice via its specific shRNA. In WT mice, C/EBPβ closely coupled with its downstream targets ApoE and AEP, with both of them strongly reduced in C/EBPβ+/− mice and substantially eradicated in C/EBPβ−/− mice, as compared to C/EBPβ+/+ mice. In addition, AEP was strongly activated in 3xTg mice, and associated with robust APP N585 and Tau N368 proteolytic cleavage, all of which were reduced in 3xTg/C/EBPβ+/− mice and completely blunted in 3xTg/C/EBPβ−/− mice. Both APP and Tau were more highly overexpressed in 3xTg mice than in WT mice, and other biochemical effects were mainly more robust in 3xTg mice as compared to their counterparts. We basically made the similar observations in 5xFAD mice, and knockdown of C/EBPβ greatly abrogated these biochemical events (Fig. 3A). qRT-PCR analysis demonstrated that C/EBPβ tightly coupled with *Apoe* mRNA levels with 3xTg and 5xFAD more abundant than WT mice (Fig. 3B). IF co-staining on the hippocampal sections from these mice principally echoed what we observed in immunoblottings. Eradicating C/EBPβ reduced both ApoE and AEP expression in both 3xTg and 5xFAD mice (Fig. 3C). IHC staining with anti-Aβ showed that the number of senile plaques in both the cortex and hippocampus were decreased in both 3xTg and 5xFAD mice as C/EBPβ gene doses were attenuated (Supplementary Fig. 8A). Moreover, IF co-staining with antibodies against AT8 and ApoE demonstrated that p-Tau and ApoE signals, respectively, were diminished in 3xTg/C/EBPβ+/− mice versus 3xTg mice, and they were substantially eliminated in 3xTg/C/EBPβ−/− mice. Again, knockdown of C/EBPβ pronouncedly repressed both of them in 5xFAD mice (Supplementary Fig. 8B).

ApoE is a major cholesterol carrier in the brain, and dysregulation of cholesterol metabolism is implicated in AD pathogenesis. The possible association between ApoE lipidation and AD risk has also been proposed. To assess whether C/EBPβ mediates ApoE lipidation, we isolated the PBS-soluble fractions from 3-month-old WT and C/EBPβ+/− mice cortex and analyzed with native PAGE gel via immunoblotting. Quantification of highly lipidated ApoE-containing particles showed that C/EBPβ knockdown decreased lipidation of ApoE in the brain (Supplementary Fig. 9A, B). Interestingly, activating LXR or retinoid X receptor (RXR) receptor with their specific small molecular agonists selectively increased both C/EBPβ and ApoE levels in WT mice, which was abolished in C/EBPβ+/− mice (Supplementary Fig. 9C, D), suggesting that LXR/RXR agonists-induced ApoE production via upregulating C/EBPβ. Hence, C/EBPβ plays an essential role in mediating ApoE expression in both 3xTg and 5xFAD mouse models, dictating AD pathogenesis.

Overexpression of C/EBPβ increases ApoE and exacerbates AD pathologies in young 3xTg mice

C/EBPβ is greatly upregulated in human AD brains [37, 43], and overexpression of C/EBPβ in young 3xTg

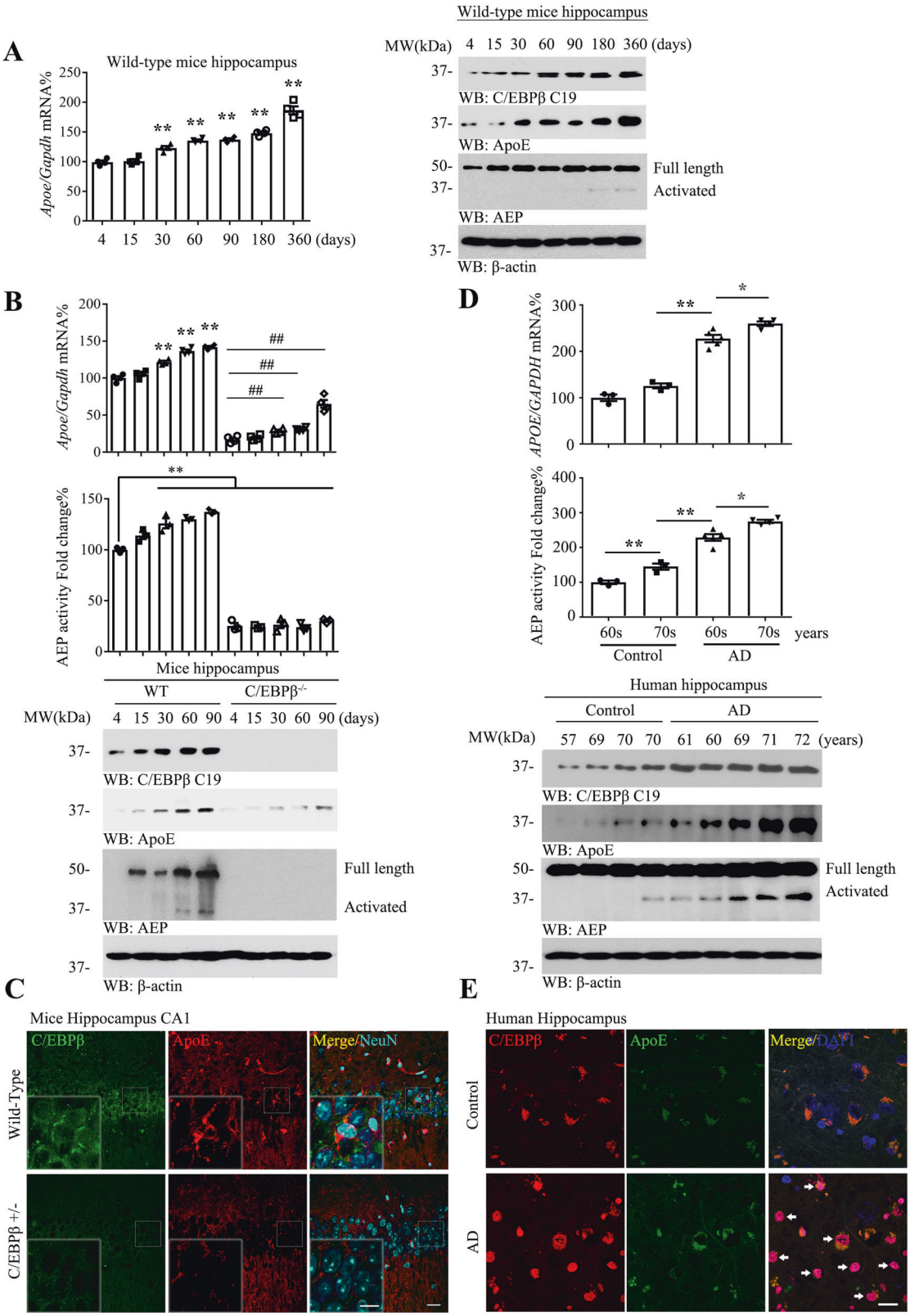

mice accelerates AD pathologies and triggers cognitive deficits [37]. To investigate the roles of ApoE in C/EBPβ-elicited AD pathologies, we injected AAV-GFP-C/EBPβ into the hippocampus of 3 months old 3xTg mice. In 1 week, the mice were treated with i.p. (twice/week) administration of control IgG or mouse monoclonal

◀ **Fig. 2 C/EBPβ regulates ApoE expression in an age-dependent manner. A** Real-time PCR and western blot were conducted from the different ages of wild-type mice hippocampus (mean ± SEM, $*P < 0.05$, $**P < 0.01$ compared with group 4 days, $n = 4$, one-way ANOVA and Bonferroni's multiple comparison test). **B** Real-time PCR, AEP activity, and western blot were conducted from the different ages of wild-type and C/EBPB$^{-/-}$ mice hippocampus (mean ± SEM, $**P < 0.01$ compared with each first group, $\#\#P < 0.01$, $n = 4$, one-way ANOVA and Bonferroni's multiple comparison test). **C** 6-month-old wild-type and C/EBPB$^{+/-}$ mice hippocampus CA1 slices were analyzed by immunofluorescence assay (green: C/EBPβ, red: ApoE, indigo: NeuN, internal scale bar: 10 μm; External scale bar: 20 μm). **D** Real-time PCR, AEP activity and western blot were conducted from the different ages of human controls and AD patients' hippocampus. Data represented 3–5 tissues/each from control 60 s ($n = 3$), control 70 s ($n = 3$), AD 60 s ($n = 5$), and AD 70 s ($n = 4$) (mean ± SEM, $*P < 0.05$, $**P < 0.01$, two-way ANOVA and Bonferroni's post hoc test, human sample information in Table S1). **E** Human ageing controls and AD patients' hippocampus slices were analyzed by the immunofluorescence assay (arrows showed the C/EBPβ in the nuclear, red: C/EBPβ, green: ApoE, blue: DAPI, scale bar: 20 μm).

antibody against mouse ApoE for consecutive 14 weeks. ApoE antibody specificity (HJ 6.3) was verified using tissues from an ApoE KO mouse (Supplementary Fig. 10F). As an alternative approach to further interrogate ApoE's pathological roles, we co-injected both AAV-GFP-C/EBPβ in the presence of control AAV or AAV-shRNA of ApoE, respectively, into the hippocampus of 3-month-old 3xTg mice. In 3 months, we found that GFP-C/EBPβ overexpression induced prominent ApoE proteins, which were totally eliminated by its specific antibody or shRNA (Fig. 4A, top and 3rd panels). qRT-PCR showed that C/EBPβ-induced *Apoe* mRNAs were significantly repressed by its shRNA (Supplementary Fig. 10A). Accordingly, AEP expression was increased and it was proteolytically activated, when GFP-C/EBPβ was overexpressed. Noticeably, anti-ApoE treatment blocked AEP activation as compared to control IgG, though AEP was also highly augmented. Remarkably, knocking down ApoE with its shRNA repressed both transfected GFP-C/EBPβ and endogenous C/EBPβ expression, leading to vigorous suppression of AEP (Fig. 4A, 2nd panel). It is worth noting that both APP and Tau expression levels were also markedly reduced, when 3xTg mice were treated with anti-ApoE or infected with shRNA of ApoE, as were levels of AEP-truncated APP N585 and Tau N368 fragments (Fig. 4A, 4th-bottom panels). These findings indicate that ApoE may interfere with AEP activation, as AEP enzymatic activities are correlated with both APP and Tau truncates (Fig. 4B). Aβ ELISA analysis revealed that removal of ApoE either with antibody or its shRNA pronouncedly decreased $A\beta_{40}$ and $A\beta_{42}$ production in the brains (Fig. 4C). Consequently, IHC and Thioflavin-S (ThS) co-staining validated that the aggregated amyloid deposits were substantially wiped out (Fig. 4D, E). Quantitative analysis also indicated that pro-inflammatory cytokines including IL-1β, IL-6, and TNFα were all attenuated in the brains, when ApoE was eliminated (Supplementary Fig. 10B). Golgi staining showed that the dendritic spines in 3xTg hippocampal neurons were strongly reduced by GFP-C/EBPβ, and these were restored when ApoE was eradicated by its monoclonal antibody or shRNA (Supplementary Fig. 10C). Electronic microscopy (EM) revealed the similar observations that removal of ApoE greatly increased the synapses in 3xTg brains (Supplementary Fig. 10D).

The LTP of fEPSP in the hippocampal CA1 region represents the molecular basis of learning and memory. Electrophysiological analysis found that the input/output ratio was suppressed and the averaged fEPSP slope was largely reduced in GFP-C/EBPβ/3xTg transgenic mice compared to control 3xTg mice, suggesting that synaptic transmission is impaired by C/EBPβ overexpression in 6-month-old 3xTg transgenic mice, but this defect was rescued by anti-ApoE antibody or ApoE gene deletion (Fig. 4F, G). Quantification of fEPSP potentiation from the final 10 min of recordings was included in Fig. 4H. Next, we examined the effect of eliminating ApoE on memory functions of 3xTg transgenic mice in the Morris water maze (MWM). During the training phase, the latency to find the platform was gradually increased in GFP-C/EBPβ/3xTg transgenic mice, demonstrating a learning effect, albeit they were markedly impaired compared to control 3xTg or ApoE-cleared GFP-C/EBPβ/3xTg mice. However, ApoE antibody treatment or its gene deletion had greatly mitigated the learning deficits compared to control IgG or control shRNA-treated mice (Supplementary Fig. 10E left panel). A probe trail revealed that elimination of ApoE in GFP-C/EBPβ/3xTg mice improved memory retention, as illustrated by the shorter latency and higher percentage of time spent in the target quadrant (Fig. 4I, J). All groups of animals exhibited equivalent swim speeds (Supplementary Fig. 10E right panel), indicating that antibody treatment or the genetic manipulations did not have any adverse effects on motor functions. Similar results were found with cued and contextual fear conditioning, which test hippocampal-independent and -dependent associative learning and memory, respectively (Fig. 4K, L). Therefore, our data strongly support that C/EBPβ-induced AD pathologies in young 3xTg mice is mediated via upregulating *Apoe* mRNA transcription and protein expression, and removal of ApoE significantly alleviates AD pathologies and rescues cognitive impairment in these mice.

Knockout of C/EBPβ in 3xTg mice diminishes AD pathologies, restored by human ApoE4 but not ApoE3

To delineate whether ApoE removal-elicited C/EBPβ reduction and subsequent amelioration of AD pathologies in

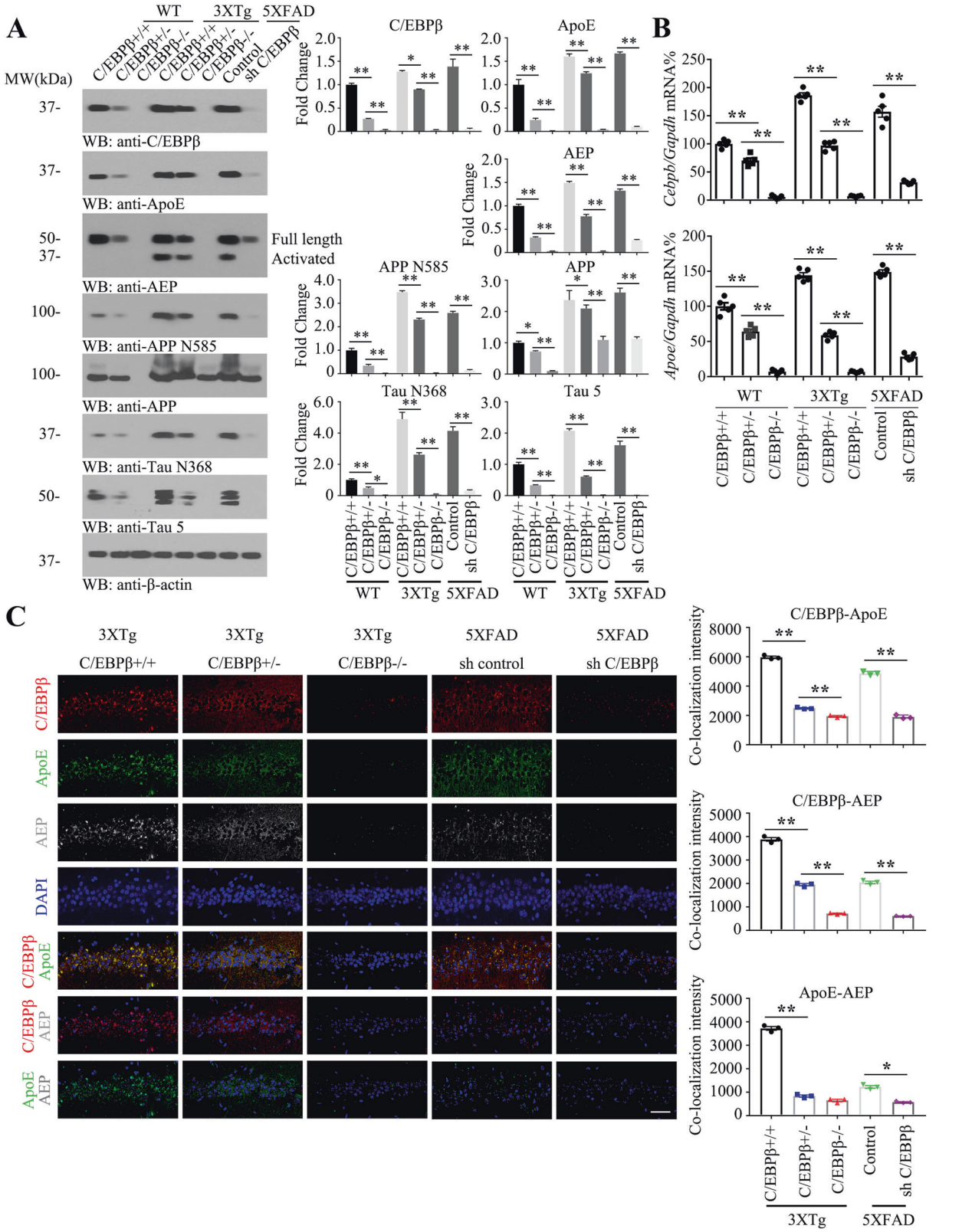

GFP-C/EBPβ/3xTg mice is indeed specifically mediated by ApoE elimination, we reasoned whether giving back ApoE in 3xTg/C/EBPβ+/− mice will reconstitute the AD pathologies and cognitive disorders. Since C/EBPβ−/− mice display some severe metabolic dysfunctions and are difficult to breed [40, 44], therefore, we chose 3xTg/C/

◀ **Fig. 3 Downregulation of C/EBPβ reduces ApoE and ameliorates APP and Tau proteolytic cleavage in AD mice.** C/EBPβ$^{+/+}$, C/EBPβ$^{+/-}$, C/EBPβ$^{-/-}$; 3xTg, 3xTg/C/EBPβ$^{+/-}$ and 3xTg/C/EBPβ$^{-/-}$ mice (6 months old); viral injection of empty vector control or sh-C/EBPβ into 5XFAD mice for 2 months (6 months old). **A** The hippocampal tissues were analyzed by immunoblotting (left panel), and quantitation of western blot data. Data represent mean ± SEM ($n = 3$, $^{*}P < 0.05$, $^{**}P < 0.01$, one-way ANOVA and Bonferroni's multiple comparison test in three groups, two-tailed student's t test in two groups, right panel). **B** Downregulation of C/EBPβ decreased *Cebpb* and *Apoe* mRNA levels. Each mouse is analyzed three times and the averaged values are plotted and subjected to statistical analyses ($n = 5$ mice/group, mean ± SEM, $^{**}P < 0.01$, one-way ANOVA and Bonferroni's multiple comparison test). **C** 3xTg, 3xTg/C/EBPβ$^{+/-}$ and 3xTg/C/EBPβ$^{-/-}$ mice (6 months old); viral injection of control or sh-C/EBPβ into 5XFAD mice for 2 months (6 months old) hippocampus slices were analyzed by the immunofluorescence assay (red: C/EBPβ, green: ApoE, gray: AEP, blue: DAPI, scale bar: 40 μm, left panel). Quantification of C/EBPβ-ApoE, C/EBPβ-AEP, ApoE-AEP co-localization intensities. Data are shown as mean ± SEM ($n = 3$ mice/group, $^{*}P < 0.05$, $^{**}P < 0.01$, one-way ANOVA and Bonferroni's multiple comparison test in three groups, two-tailed student's t test in two groups). See also Supplementary Figs. 8 and 9.

EBPβ+/− instead of 3xTg/C/EBPβ−/− mice to address these questions. Accordingly, we employed 3 months old of C/EBPβ+/+,+/− mice and 3xTg/C/EBPβ+/+, 3xTg/C/EBPβ+/− mice, and injected AAV-ApoE3 or AAV-ApoE4 into the hippocampus of these mice, respectively. In 3 months, we found that human ApoE4 induced a more significant increase of C/EBPβ than ApoE3. Again, its downstream target AEP was also markedly increased and proteolytically activated in ApoE4 brains as compared to ApoE3 in wild-type mice. Strikingly, both APP and Tau were augmented more prominently in ApoE4-injected brains versus ApoE3. Consequently, both of them were strongly cleaved by AEP into APP N585 and Tau N368 fragments. All of these biochemical events were evidently reduced in C/EBPβ+/− mice, though both ApoE3 and ApoE4 levels were detectable in the brains with the latter more plentiful than the former. As expected, similar biochemical activities were observed in 3xTg/C/EBPβ+/+ and 3xTg/C/EBPβ+/− mice, but they were all adversely elevated and intensified compared to the corresponding counterparts. Again, 3xTg/C/EBPβ+/+ mice exhibited much more robust effects than 3xTg/C/EBPβ+/− mice (Fig. 5A). qRT-PCR indicated that both *Cebpb* and *Apoe* mRNA concentrations displayed the similar pattern with ApoE4 more profuse than ApoE3 in wild-type C/EBPβ versus its heterozygous mice (Supplementary Fig. 11A). Consequently, both $A\beta_{40}$ and $A\beta_{42}$ levels in these mice demonstrated the same format, fitting with AEP enzymatic activities (Fig. 5B, C). Remarkably, IHC analysis with anti-Aβ showed that ApoE4 triggered significantly more amyloid deposits than ApoE3 in wild-type mice, and these aggregates were almost undetectable in C/EBPβ+/− mice. Once more, IHC and ThS co-staining disclosed the same results for amyloid plaques (Fig. 5D, E). Quantification of the inflammatory cytokines showed that IL-1β, IL-6, and TNFα levels tightly correlated with the scales of amyloid inclusions (Supplementary Fig. 11B). Golgi staining and EM analysis indicated that the dendritic spines and synapses were inversely coupled to Aβ concentrations in the brains (Supplementary Fig. 11C, D). Electrophysiology revealed that LTP was consistent with the synapse densities, suggesting that human ApoE4 attenuated the synaptic plasticity more substantively than ApoE3, with wild-type mice more severe versus C/EBPβ+/− mice. The same pattern occurred to 3xTg and 3xTg/C/EBPβ+/− mice (Fig. 5F–H).

To explore whether manipulation of ApoE and C/EBPβ+/− affects cognitive impairment in 3xTg mice, we tested spatial learning and memory using the MWM. More serious deficits were observed in ApoE4-injected 3xTg mice than ApoE3. However, the performance of 3xTg/C/EBPβ+/− mice remained comparable, no matter whether ApoE3 or E4 was administrated. Again, human ApoE4-injected wild-type mice displayed decreased memory compared to ApoE3 mice, and these defects were diminished in C/EBPβ+/− mice (Fig. 5I, J and Supplementary Fig. 11E). Similar results were observed with cued and contextual fear conditioning (Fig. 5K, L). Together, these behavioral tests support that overexpression of human ApoE4 in 3xTg/C/EBPβ+/− mice restores AD pathologies and cognitive defects.

C/EBPβ preferentially promotes more ApoE expression in human neurons when the allele is ApoE4 versus ApoE3

The Apoε4 allele frequency is about 15% in the general population but is 40% in AD patients [6]. To investigate whether C/EBPβ selectively upregulates ApoE ε4 versus ε3 in human AD brains, we conduced qRT-PCR and immunoblotting to examine their relationship. Interestingly, *CEBPB* mRNA was more abundant in human AD brains with Apo ε4/ε4 than Apo ε3/ε3, and Apo ε4/ε4 mRNA levels were significantly higher than those of Apo ε3/ε3 (Fig. 6A). Consistently, C/EBPβ proteins were much more copious in human AD brains with Apo ε4/ε4 than Apo ε3/ε3, so were the active p-C/EBPβ T235. Accordingly, ApoE protein concentrations were enriched in Apo ε4/ε4 versus Apo ε3/ε3. AEP, the downstream target of C/EBPβ, echoed with C/EBPβ levels. Active AEP robustly cleaved more APP N585 and Tau N368 in Apo ε4/ε4 than Apo ε3/ε3 (Fig. 6B, C). To assess whether C/EBPβ preferentially mediates ApoE allele expression in human neurons, we induced human ApoE ε4/ε4 and ApoE ε3/ε3 iPSCs into neurons that were validated by neuronal markers MAP2 and NeuN (Fig. 6D). Again, *CEBPB* mRNA was more lavish in ApoE ε4/ε4 neurons than ApoE ε3/ε3, and ApoE ε4/ε4

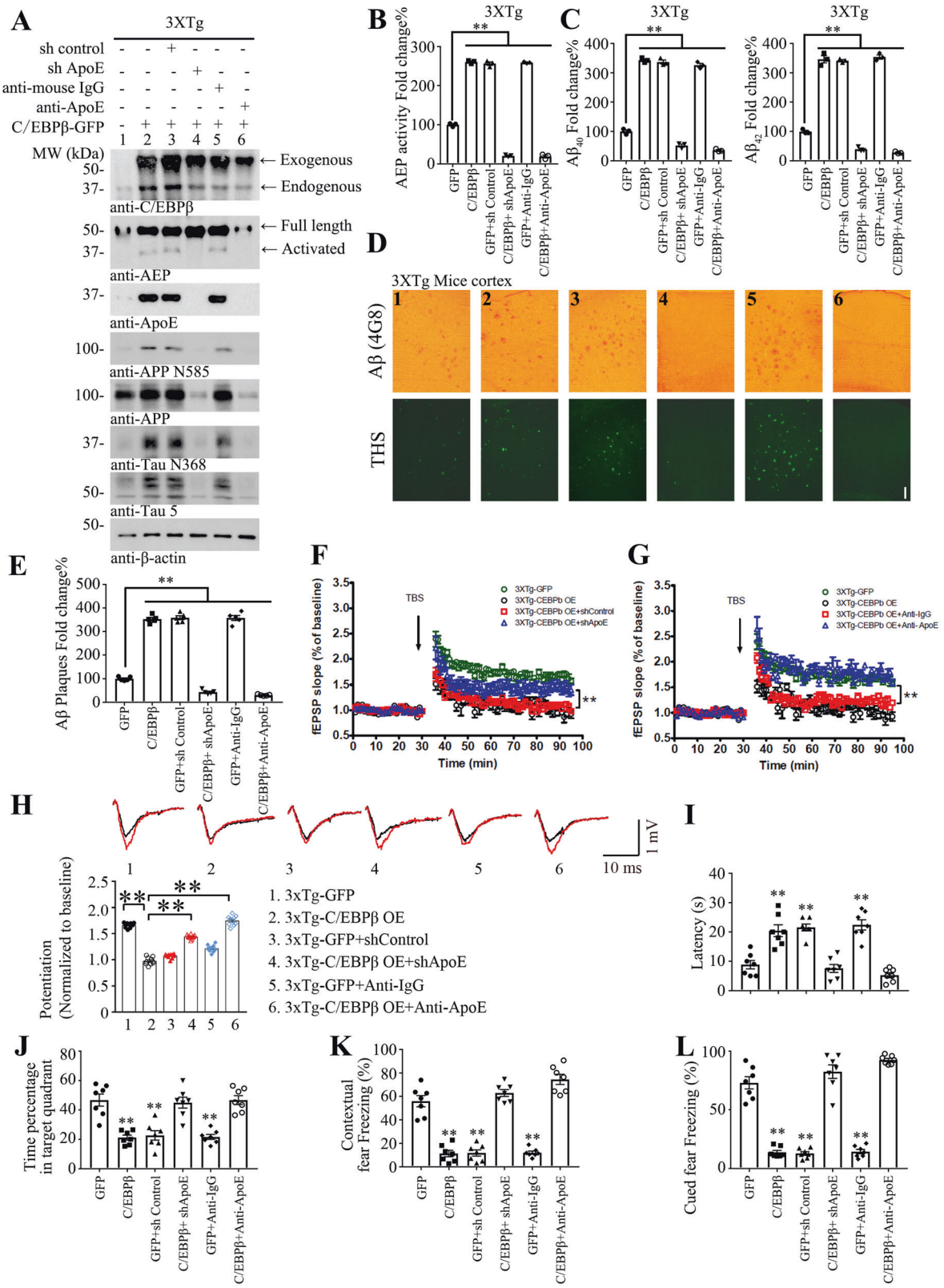

mRNA concentrations were significantly higher than ApoE ε3/ε3 in these human neurons. Overexpression of GFP-C/EBPβ in these neurons leds to both ApoE ε4/ε4 and ε3/ε3 mRNA upregulation with the former higher than the latter as compared to control GFP. On the other hand, depletion of C/EBPβ strongly diminished both ApoE ε4/ε4 and ε3/ε3

◀ **Fig. 4 Overexpression of C/EBPβ in young 3XTg mice accelerates the onset of AD pathogenesis and cognitive dysfunction by upregulating ApoE.** 2 months old 3XTg mice stereotactic injected with control or C/EBPβ lentivirus for 3 months, and two groups were treated with sh-control or sh-ApoE virus, the other two groups were treated with intraperitoneal injection of anti-IgG or anti-ApoE at the same time. **A** The hippocampal tissues were analyzed by immunoblotting ($n = 3$ mice per group). **B, C** Overexpression of C/EBPβ increased the activity of AEP and expression of Aβ in an ApoE-dependent way. Each mouse is analyzed three times and the averaged values are plotted and subjected to statistical analyses ($n = 3$ mice/group, mean ± SEM, $^{**}P < 0.01$, two-way ANOVA and Bonferroni's post hoc test). **D** Overexpression of C/EBPβ improved the formation of amyloid plaques in young 3xTg mice, and downregulation of ApoE decreased the Aβ inclusions, co-staining with Aβ and THS, scale bar: 100 μm. **E** Quantification from both 4G8 and THS-positive signals, $n = 5$, 2 mice/group, 2–3 slices/mouse (mean ± SEM, $^{**}P < 0.01$, two-way ANOVA and Bonferroni's post hoc test). **F, G** Electrophysiology analysis. C/EBPβ overexpression worsened the LTP defects in 3xTg mice. LTP of fEPSPs (mean ± SEM; $n = 6$ in each group; $^{*}P < 0.05$ compared with 3xTg-control, two-way ANOVA and Bonferroni's post hoc test). Shown traces were representative fEPSPs of ten samples recorded before and after TBS (theta-burst stimulation). **H** Quantification of fEPSP potentiation from the final 10 min of recordings (86–95 min in Fig. 5G, H) normalized to basal levels. Representative recording traces: black line, baseline; red line, LTP 86–95 min (mean ± SEM; $n = 6$ in each group; $^{*}P < 0.05$ compared with 3xTg-control, two-way ANOVA and Bonferroni's post hoc test). **I, J** Morris water maze analysis. C/EBPβ overexpression exacerbated the learning and memory dysfunctions, and downregulation of ApoE reversed the cognitive dysfunctions (mean ± SEM; $n = 7$–8 mice per group; $^{*}P < 0.05$ compared with group 1, two-way ANOVA and Bonferroni's post hoc test). **K, L** Fear condition tests. Contextual and cued fear conditions were reduced in C/EBPβ overexpressed mice. Downregulation of ApoE reversed the memory deficits (mean ± SEM; $n = 7$–8 mice per group; $^{*}P < 0.05$ compared with group 1, two-way ANOVA and Bonferroni's post hoc test). See also Supplementary Fig. 10.

expression (Fig. 6E). Immunoblotting observations were tightly coupled with qRT-PCR results with AEP more highly activated in ApoE ε4/ε4 neurons than ApoE ε3/ε3 (Fig. 6F, G). Thus, these data strongly support that C/EBPβ favorably escalates ApoE ε4/ε4 expression versus ApoE ε3/ε3 in human neurons and AD patients.

Discussion

The risk for AD is associated with the APOE allele (ε4 > ε3 > ε2), and inheritance of one or two copies of APOE ε4 dramatically increases the late-onset AD risk, ~3- or 12-fold, respectively [45]. Individuals with two copies of the ApoE4 allele have an increased risk for sporadic or familial AD, with a significantly lower age of onset compared with AD patients not carrying this allele [42, 46, 47]. Despite intensive research efforts that have revealed several important insights regarding ApoE4's role in AD pathophysiology, a major unanswered question is the mechanism by which ApoE4 confers AD risk [48]. ApoE-lipoproteins bind to several cell-surface receptors to deliver lipids, and also to hydrophobic Aβ peptide, which is thought to initiate toxic events that lead to synaptic dysfunction and neurodegeneration in AD. ApoE isoforms differentially regulate Aβ aggregation and clearance in the brain, and have distinct functions in regulating brain lipid transport, glucose metabolism, neuronal signalings, neuro-inflammation, and mitochondrial function [17]. In addition to its effects on APP processing and signaling, ApoE4 but not ApoE3 triggers a marked reduction in the expression of SirT1, a NAD-dependent protein deacetylase, which has been linked to the normal aging process and also suppresses AD-related biochemical events, in cultured neural cells, cerebrospinal fluid, and in the brains of patients with AD [49, 50].

We showed here that expression of both C/EBPβ and ApoE gradually increase during ageing in wild-type mouse brains and KO of C/EBPβ substantially eliminated ApoE expression in their brains (Fig. 2A, B). We also observed that both *APOE* mRNA and protein levels were significantly elevated in AD patient brains compared to healthy controls, fitting with prominently augmented C/EBPβ in AD patient brains (Fig. 2D, E). These findings are consistent with previous studies that reported increased expression of *APOE* mRNA in the frontal and temporal cortex [51, 52] and the hippocampus [53] of patients with neuropathologically confirmed AD. Levels of both *APOE* mRNA and protein are raised, presumably owing to an increase in ApoE expression within reactive astrocytes, a neuropathological hallmark of AD [54–56]. Nevertheless, it has also been reported that ApoE levels in CSF and plasma tend to be lower in AD patients than in healthy individuals, although such findings remain controversial [57, 58]. Thus, it has been proposed that increasing the expression of ApoE in all *APOE* genotypes may prevent or slow progression of AD through acceleration of Aβ metabolism and promotion of ApoE functions in lipid metabolism and synaptic support. For instance, Cramer et al. reported that stimulation of *APOE* transcriptional expression with RXR agonist bexarotene triggers Aβ clearance and improves cognitive activities [59]. Nonetheless, our findings do not support this conclusion. We showed that human ApoE4 but not ApoE3 overexpression aggravates AD pathologies in a C/EBPβ-dependent manner (Fig. 5 and Supplementary Figs. 10 and 11).

It is worth noting that ApoE elimination decreases both C/EBPβ and its downstream transcriptional target AEP levels. Surprisingly, both APP and Tau expressions were also robustly attenuated in GFP-C/EBPβ-3xTg mice after ApoE depletion (Fig. 4). These findings suggest that removal of ApoE, the downstream effector of C/EBPβ, somehow inhibits its transcriptional activity. Probably, ApoE might feed-back and stimulate C/EBPβ transcriptional activity, which simultaneously regulates numerous

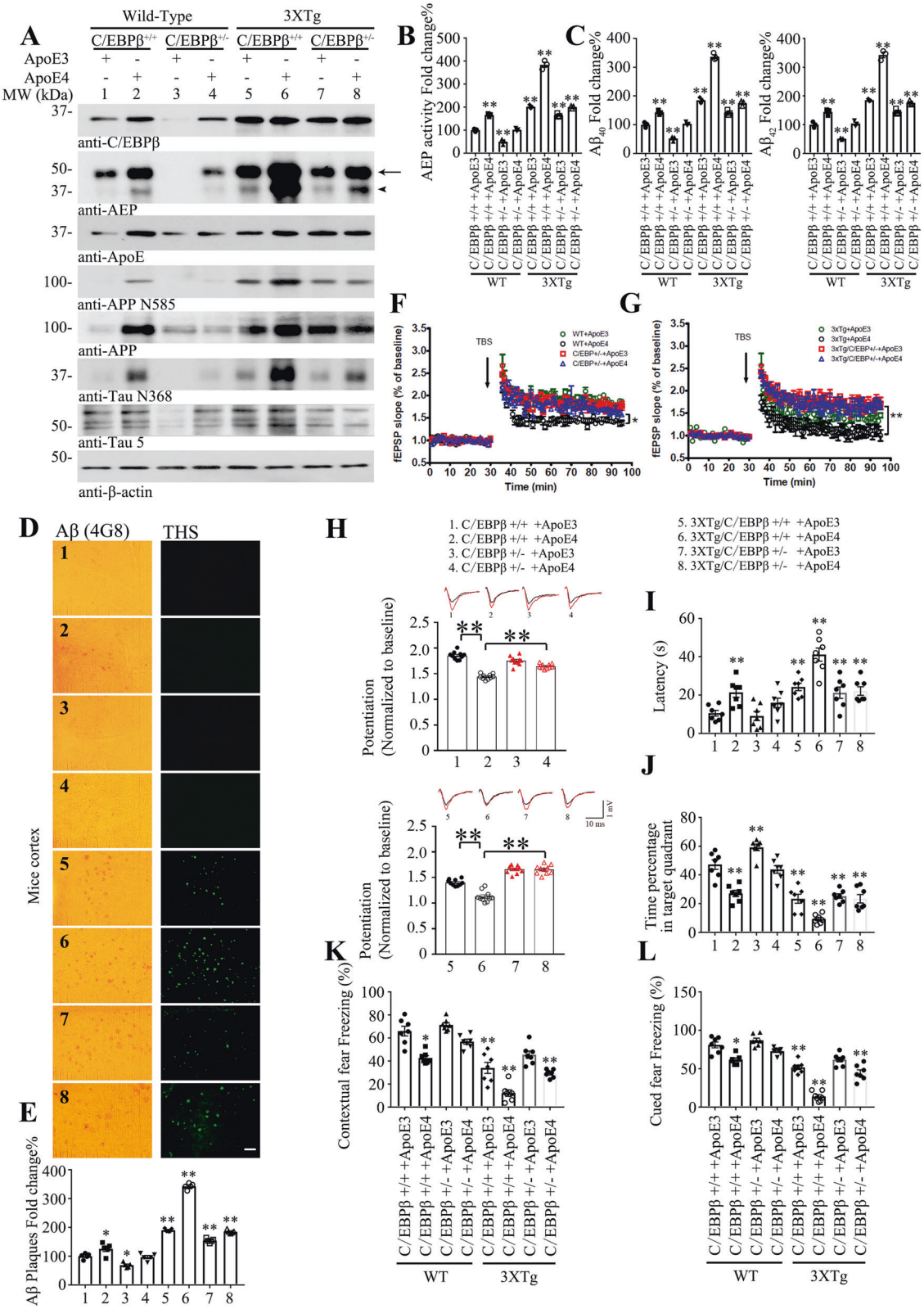

AD genes' expression including *APP, MAPT* (Tau), and *LGMN* (AEP). For instance, it has been reported before that C/EBPβ may modulate *APP* mRNA transcription in PC12 cells [60]. We have recently shown that C/EBPβ binds to *LGMN* promoter and regulates its mRNA transcription during aging [37]. Conceivably, eradication of

◀ **Fig. 5 Overexpression of ApoE4 reconstitutes AD pathologies and restores the cognitive impairments in 3xTg/C/EBP+/− mice.** Viral injection of ApoE3 or ApoE4 into C/EBPβ$^{+/+}$; C/EBPβ$^{+/−}$; 3xTg and 3xTg/C/EBPβ$^{+/−}$ mice (3 months old) for 3 months. **A** The hippocampal tissues were analyzed by immunoblotting ($n = 2$ mice per group, arrow: full-length AEP, arrowhead: activated AEP). **B, C** Overexpression of ApoE4 increased the activity of AEP and expression of Aβ. Each mouse is analyzed three times and the averaged values are plotted and subjected to statistical analyses ($n = 3$ mice/group, mean ± SEM, $^{**}P < 0.01$, two-way ANOVA and Bonferroni's post hoc test). **D** ApoE4 overexpression enhanced the early formation of amyloid plaques in wild-type or 3xTg mice, and downregulation of C/EBPβ decreased Aβ aggregates, co-staining with Aβ and THS, Scale bar: 100 μm. **E** Quantification from both 4G8 and THS-positive signals, $n = 5$, 2 mice/group, 2–3 slices/mouse (mean ± SEM, $^{*}P < 0.05$, $^{**}P < 0.01$ vs. group 1, two-way ANOVA and Bonferroni's post hoc test). **F, G** Electrophysiology analysis. ApoE4 overexpression worsened the LTP defects in wild-type or 3xTg mice. LTP of fEPSPs (mean ± SEM; $n = 6$ in each group; $^{*}P < 0.05$, $^{**}P < 0.01$ compared with group1, two-way ANOVA and Bonferroni's post hoc test). Shown traces were representative fEPSPs of ten samples recorded before and after TBS (theta-burst stimulation). **H** Quantification of fEPSP potentiation from the final 10 min of recordings (86–95 min in Fig. 4G, H) normalized to basal levels. Representative recording traces: black line, baseline; red line, LTP 86–95 min (mean ± SEM; $n = 6$ in each group; $^{*}P < 0.05$ compared with 3xTg-control, two-way ANOVA and Bonferroni's post hoc test). **I, J** Morris water maze analysis. ApoE4 overexpression exacerbated the learning and memory dysfunctions (mean ± SEM; $n = 7$–8 mice per group; $^{*}P < 0.05$ compared with group1, two-way ANOVA and Bonferroni's post hoc test). **K, L** Fear condition tests. Contextual and cued fear conditions were reduced in ApoE overexpressed mice. (Mean ± SEM; $n = 7$–8 mice per group; $^{*}P < 0.05$, $^{**}P < 0.01$ compared with group1, two-way ANOVA and Bonferroni's post hoc test). See also Supplementary Fig. 11.

ApoE antagonizes its stimulatory effect on C/EBPβ. This hypothesis was supported by our human ApoE3 and ApoE4 overexpression experiments in 3xTg and 3xTg/C/EBP+/− mice (Fig. 5). Although both AAV-ApoE3 and ApoE4 viruses possess the comparable titers and infectious potency, ApoE4 expression levels were much higher than ApoE3 in C/EBPβ+/+ mice than C/EBPβ+/− mice (Fig. 5). Accordingly, overexpression of ApoE4 in SH-SY5Y cells or treating primary neurons with recombinant ApoE4 proteins robustly activated C/EBPβ and p-C/EBPβ, leading to AEP upregulation and activation that subsequently cleaved both APP and Tau (Supplementary Fig. 12A). Notably, the inflammatory cytokines were also significantly elevated by ApoE4 as compared to ApoE3, so were the mRNAs of *Cebpb, LGMN, APP* and *MAPT* genes and AEP enzymatic activities in primary neurons (Supplementary Fig. 12B–D). Remarkably, depletion of LRP, a major ApoE receptor in the plasma membrane, greatly antagonized ApoE4's biological effects in primary neurons (Supplementary Fig. 13). Therefore, C/EBPβ was selectively activated by ApoE4 but not E3, resulting in the positive feed-forward to amplify ApoE expression. Conceivably, there is a feedback loop between C/EBPβ and ApoE4. ApoE4 enhances neuro-inflammation and escalates Aβ, and both activate C/EBPβ [28, 36]. In the current study, we show that C/EBPβ acts as a crucial transcription factor for ApoE via binding to its promoter in different cell types. On the other hand, ApoE4 may stimulate neuro-inflammation and escalate Aβ to activate C/EBPβ [28, 36].

ApoE4 seems to have pro-inflammatory and/or reduced anti-inflammatory functions, which could further aggravate AD pathology. Correspondingly, ApoE removal with its specific antibody or deletion with its shRNA substantively alleviated the inflammation in GFP-C/EBPβ overexpressed 3xTg mice (Supplementary Fig. 10B). It has been reported that Aβ activates C/EBPβ[36]. Markedly, overexpression of human ApoE4 but not ApoE3 aggravates neuro-inflammation in C/EBPβ-dependent way in both wild-type mice and 3xTg mice (Supplementary Fig. 11B), underscoring that the crosstalk between C/EBPβ and ApoE4 mutually regulates each other in the vicious cycle to amplify the neuro-inflammation. Consistent with our findings, it has been reported that C/EBPα binds to the porcine *APOE* promoter and regulates its gene expression [61]. Nonetheless, we discovered that C/EBPβ but not C/EBPα isoform specifically mediated human or mouse ApoE gene expression (Fig. 1 and Supplementary Figs. 2, 3). Interestingly, several studies have now demonstrated an indirect role of ApoE4 in gene transcription. For instance, ApoE4 may act like a signaling molecule by increasing the nuclear translocation of histone deacetylases (HDACs) in human neurons that in turn reduce BDNF expression, in comparison to ApoE3, which increases histone-3 acetylation and upregulates BDNF expression [62]. In another recent study using human neurons derived from ES cells, Huang et al. showed that ApoE4 robustly stimulates APP transcription and Aβ production by activating a non-canonical MAP kinase pathway involving DLK, MKK7, and ERK1/2. This cascade finally stimulates c-Fos phosphorylation and APP gene transcription, leading to increased APP and Aβ synthesis [8]. Strikingly, we found that C/EBPβ selectively escalates ApoE4 expression versus ApoE3 in human neurons, correlating with more abundant ApoE protein levels in AD patients with ApoE4/4 as compared to ApoE3/3. In alignment with these findings, C/EBPβ is more phosphorylated and activated in the former than the latter (Fig. 6). Taken together, we provide extensive evidence to support that C/EBPβ acts as a specific *APOE* gene transcription factor and dictates its expression during aging and in human AD. Clearly, our data support the notion that C/EBPβ may act as a major AD pathology driver via simultaneously upregulating AEP and ApoE (Fig. 6H). AEP, ApoE clearance remarkably

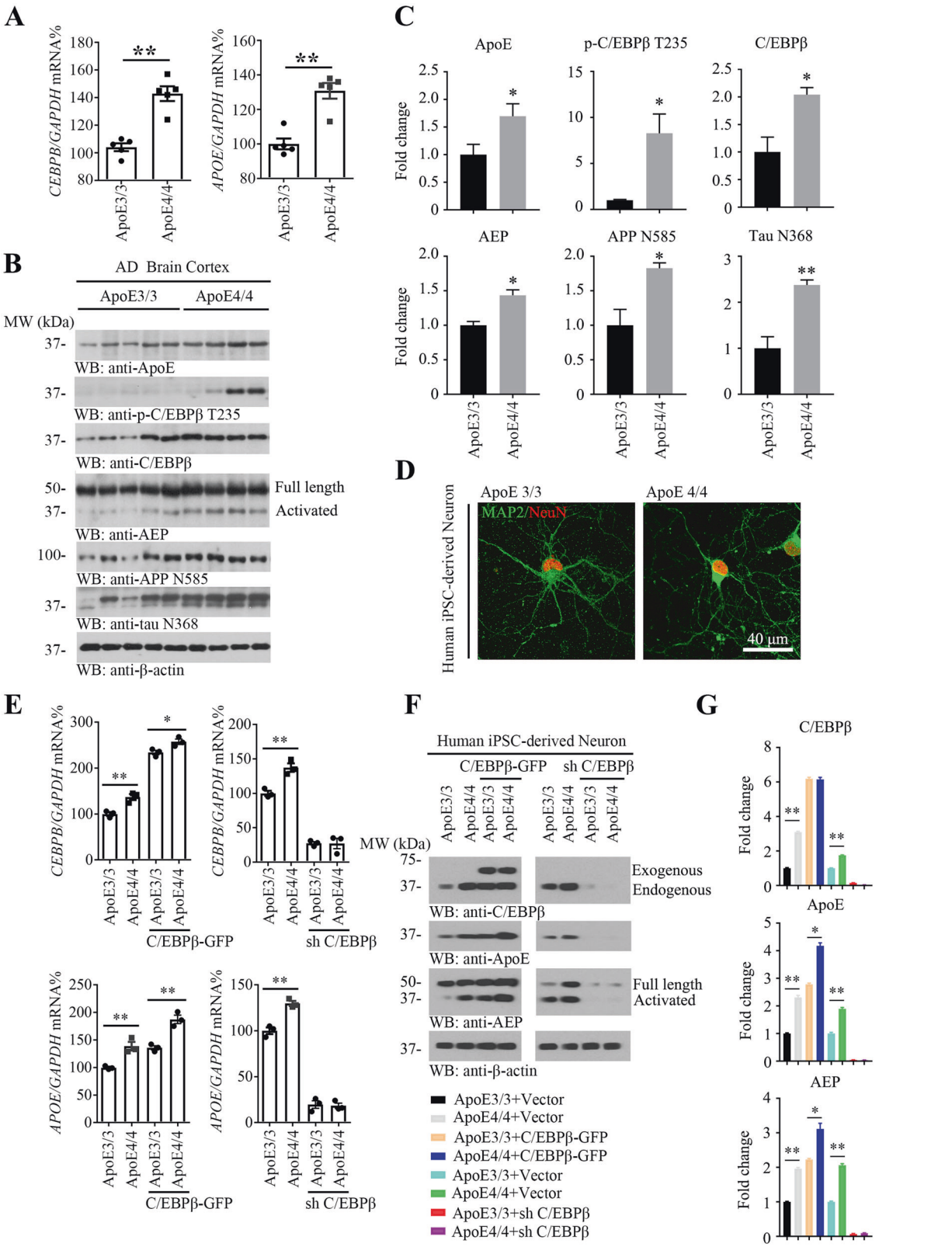

attenuates C/EBPβ-triggered AD pathological effects. Notably, C/EBPβ and ApoE mutually regulate each other and amplify their biological roles in AD pathogenesis (Supplementary Fig. 14). Conceivably, disruption of this vicious cycle might provide an attractive strategy for blocking AD onset and progression.

◀ **Fig. 6 Interactions between C/EBPβ and APOE genotypes in human brain and iPSC-derived neurons. A** AD patients with ApoE4/4 genotype showed higher *CEBPB* and *APOE* mRNA level than ApoE3/3. Data represented 4–5 independent experiments (mean ± SEM, $^{**}P < 0.01$, two-tailed student's *t* test). **B** The AD patients' brain cortex tissues were analyzed by immunoblotting. C/EBPβ and its active p-C/EBPβ T235 signals were selectively escalated in ApoE4/4 AD brains versus ApoE3/3 brains. **C** Quantitation of western blot data. Data represent mean ± SEM ($n = 4$–5, $^{*}P < 0.05$, $^{**}P < 0.01$, two-tailed student's *t* test). **D** The human iPSC-derived neurons from ApoE3/3 or ApoE4/4 genotype were stained for NeuN (red) and MAP2 (green) after cultured for 28 days, scale bar: 40 μm. **E, F** The human iPSC-derived neurons were treated with lentivirus over-expressing or knocking down C/EBPβ for 7 days, respectively. *CEBPB* and *APOE* mRNA levels in induced human neurons were detected by qPCR (mean ± SEM, $n = 3$, $^{*}P < 0.05$, $^{**}P < 0.01$, two-way ANOVA and Bonferroni's post hoc test) (**E**), and ApoE and AEP protein levels were detected by western blot (**F**). **G** Quantitation of western blot data. Data represent mean ± SEM ($n = 3$, $^{*}P < 0.05$, $^{**}P < 0.01$, two-way ANOVA and Bonferroni's post hoc test).

Acknowledgements This work is supported by a grant from the National Institute of Health (RF1, AG051538; RO1, AG065517) to KY, the State Key Program of National Natural Science Foundation of China (No. 31771114) to X-CW. The China Postdoctoral Science Foundation (2019T120662) to YX. The authors are thankful to Dr David Holtzman for the generous gift of anti-ApoE monoclonal antibody and critical proofreading of the manuscript. This study was supported in part by the Rodent Behavioral Core (RBC), which is subsidized by the Emory University School of Medicine and is one of the Emory Integrated Core Facilities. Additional support was provided by the Viral Vector Core of the Emory Neuroscience NINDS Core Facilities (P30NS055077). Further support was provided by the Georgia Clinical and Translational Science Alliance of the National Institutes of Health under Award Number UL1TR002378.

Author contributions KY conceived the project, designed the experiments, analyzed the data, and wrote the manuscript. YX, ZW, JZ, and KY designed and performed most of the experiments and analyzed the data. XL prepared primary neurons and assisted with in vivo and in vitro experiments. SPY, J-ZW, and X-CW assisted with data analysis and interpretation and critically read the manuscript.

Compliance with ethical standards

Conflict of interest The authors declare that they have no conflict of interest.

Publisher's note Springer Nature remains neutral with regard to jurisdictional claims in published maps and institutional affiliations.

References

1. Mahley RW. Apolipoprotein E: cholesterol transport protein with expanding role in cell biology. Science. 1988;240:622–30.
2. Harold D, Abraham R, Hollingworth P, Sims R, Gerrish A, Hamshere ML, et al. Genome-wide association study identifies variants at CLU and PICALM associated with Alzheimer's disease. Nat Genet. 2009;41:1088–93.
3. Lambert JC, Heath S, Even G, Campion D, Sleegers K, Hiltunen M, et al. Genome-wide association study identifies variants at CLU and CR1 associated with Alzheimer's disease. Nat Genet. 2009;41:1094–9.
4. Chartier-Harlin MC, Parfitt M, Legrain S, Perez-Tur J, Brousseau T, Evans A, et al. Apolipoprotein E, epsilon 4 allele as a major risk factor for sporadic early and late-onset forms of Alzheimer's disease: analysis of the 19q13.2 chromosomal region. Hum Mol Genet. 1994;3:569–74.
5. Houlden H, Crook R, Backhovens H, Prihar G, Baker M, Hutton M, et al. ApoE genotype is a risk factor in nonpresenilin early-onset Alzheimer's disease families. Am J Med Genet. 1998;81:117–21.
6. Farrer LA, Cupples LA, Haines JL, Hyman B, Kukull WA, Mayeux R, et al. Effects of age, sex, and ethnicity on the association between apolipoprotein E genotype and Alzheimer disease. A meta-analysis. APOE and Alzheimer Disease Meta Analysis Consortium. JAMA. 1997;278:1349–56.
7. Corder EH, Saunders AM, Strittmatter WJ, Schmechel DE, Gaskell PC, Small GW, et al. Gene dose of apolipoprotein E type 4 allele and the risk of Alzheimer's disease in late onset families. Science. 1993;261:921–3.
8. Huang YA, Zhou B, Wernig M, Sudhof TC. ApoE2, ApoE3, and ApoE4 differentially stimulate APP transcription and Abeta secretion. Cell. 2017;168:427–41.e21.
9. Shi Y, Yamada K, Liddelow SA, Smith ST, Zhao L, Luo W, et al. ApoE4 markedly exacerbates tau-mediated neurodegeneration in a mouse model of tauopathy. Nature. 2017;549:523–7.
10. Wang C, Najm R, Xu Q, Jeong DE, Walker D, Balestra ME, et al. Gain of toxic apolipoprotein E4 effects in human iPSC-derived neurons is ameliorated by a small-molecule structure corrector. Nat Med. 2018;24:647–57.
11. Namba Y, Tomonaga M, Kawasaki H, Otomo E, Ikeda K. Apolipoprotein E immunoreactivity in cerebral amyloid deposits and neurofibrillary tangles in Alzheimer's disease and kuru plaque amyloid in Creutzfeldt-Jakob disease. Brain Res. 1991;541:163–6.
12. LaDu MJ, Falduto MT, Manelli AM, Reardon CA, Getz GS, Frail DE. Isoform-specific binding of apolipoprotein E to beta-amyloid. J Biol Chem. 1994;269:23403–6.
13. Wisniewski T, Golabek A, Matsubara E, Ghiso J, Frangione B, Apolipoprotein E. binding to soluble Alzheimer's beta-amyloid. Biochem Biophys Res Commun. 1993;192:359–65.
14. Strittmatter WJ, Weisgraber KH, Huang DY, Dong LM, Salvesen GS, Pericak-Vance M, et al. Binding of human apolipoprotein E to synthetic amyloid beta peptide: isoform-specific effects and implications for late-onset Alzheimer disease. Proc Natl Acad Sci U S A. 1993;90:8098–102.
15. Bales KR, Verina T, Dodel RC, Du Y, Altstiel L, Bender M, et al. Lack of apolipoprotein E dramatically reduces amyloid beta-peptide deposition. Nat Genet. 1997;17:263–4.
16. Irizarry MC, Rebeck GW, Cheung B, Bales K, Paul SM, Holzman D, et al. Modulation of A beta deposition in APP transgenic mice by an apolipoprotein E null background. Ann N Y Acad Sci. 2000;920:171–8.
17. Liu CC, Liu CC, Kanekiyo T, Xu H, Bu G. Apolipoprotein E and Alzheimer disease: risk, mechanisms and therapy. Nat Rev Neurol. 2013;9:106–18.
18. Mahley RW, Rall SC Jr. Apolipoprotein E: far more than a lipid transport protein. Annu Rev Genom Hum Genet. 2000;1:507–37.
19. Elshourbagy NA, Liao WS, Mahley RW, Taylor JM. Apolipoprotein E mRNA is abundant in the brain and adrenals, as well as in the liver, and is present in other peripheral tissues of rats and marmosets. Proc Natl Acad Sci USA. 1985;82:203–7.
20. Xu Q, Bernardo A, Walker D, Kanegawa T, Mahley RW, Huang Y. Profile and regulation of apolipoprotein E (ApoE) expression in the CNS in mice with targeting of green fluorescent protein gene to the ApoE locus. J Neurosci. 2006;26:4985–94.

21. Mahley RW, Weisgraber KH, Huang Y. Apolipoprotein E4: a causative factor and therapeutic target in neuropathology, including Alzheimer's disease. Proc Natl Acad Sci U S A. 2006;103:5644–51.
22. Pfrieger FW. Cholesterol homeostasis and function in neurons of the central nervous system. Cell Mol Life Sci. 2003;60:1158–71.
23. Greenbaum LE, Li W, Cressman DE, Peng Y, Ciliberto G, Poli V, et al. CCAAT enhancer-binding protein beta is required for normal hepatocyte proliferation in mice after partial hepatectomy. J Clin Invest. 1998;102:996–1007.
24. Ramji DP, Foka P. CCAAT/enhancer-binding proteins: structure, function and regulation. Biochem J. 2002;365:561–75.
25. Poli V. The role of C/EBP isoforms in the control of inflammatory and native immunity functions. J Biol Chem. 1998;273:29279–82.
26. Caivano M, Gorgoni B, Cohen P, Poli V. The induction of cyclooxygenase-2 mRNA in macrophages is biphasic and requires both CCAAT enhancer-binding protein beta (C/EBP beta) and C/EBP delta transcription factors. J Biol Chem. 2001;276:48693–701.
27. Bradley MN, Zhou L, Smale ST. C/EBPbeta regulation in lipopolysaccharide-stimulated macrophages. Mol Cell Biol. 2003;23:4841–58.
28. Cardinaux JR, Allaman I, Magistretti PJ. Pro-inflammatory cytokines induce the transcription factors C/EBPbeta and C/EBPdelta in astrocytes. Glia. 2000;29:91–7.
29. Ejarque-Ortiz A, Medina MG, Tusell JM, Perez-Gonzalez AP, Serratosa J, Saura J. Upregulation of CCAAT/enhancer binding protein beta in activated astrocytes and microglia. Glia. 2007;55:178–88.
30. Pulido-Salgado M, Vidal-Taboada JM, Saura J. C/EBPbeta and C/EBPdelta transcription factors: basic biology and roles in the CNS. Prog Neurobiol. 2015;132:1–33.
31. Straccia M, Gresa-Arribas N, Dentesano G, Ejarque-Ortiz A, Tusell JM, Serratosa J, et al. Pro-inflammatory gene expression and neurotoxic effects of activated microglia are attenuated by absence of CCAAT/enhancer binding protein beta. J Neuroinflamm. 2011;8:156.
32. Kapadia R, Tureyen K, Bowen KK, Kalluri H, Johnson PF, Vemuganti R. Decreased brain damage and curtailed inflammation in transcription factor CCAAT/enhancer binding protein beta knockout mice following transient focal cerebral ischemia. J Neurochem. 2006;98:1718–31.
33. Cortes-Canteli M, Luna-Medina R, Sanz-Sancristobal M, Alvarez-Barrientos A, Santos A, Perez-Castillo A. CCAAT/enhancer binding protein beta deficiency provides cerebral protection following excitotoxic injury. J Cell Sci. 2008;121:1224–34.
34. Lukiw WJ. Gene expression profiling in fetal, aged, and Alzheimer hippocampus: a continuum of stress-related signaling. Neurochem Res. 2004;29:1287–97.
35. Li R, Strohmeyer R, Liang Z, Lue LF, Rogers J. CCAAT/enhancer binding protein delta (C/EBPdelta) expression and elevation in Alzheimer's disease. Neurobiol Aging. 2004;25:991–9.
36. Ramberg V, Tracy LM, Samuelsson M, Nilsson LN, Iverfeldt K. The CCAAT/enhancer binding protein (C/EBP) delta is differently regulated by fibrillar and oligomeric forms of the Alzheimer amyloid-beta peptide. J Neuroinflamm. 2011;8:34.
37. Wang ZH, Gong K, Liu X, Zhang Z, Sun X, Wei ZZ, et al. C/EBPbeta regulates delta-secretase expression and mediates pathogenesis in mouse models of Alzheimer's disease. Nat Commun. 2018;9:1784.
38. Zhang Z, Song M, Liu X, Kang SS, Kwon IS, Duong DM, et al. Cleavage of tau by asparagine endopeptidase mediates the neurofibrillary pathology in Alzheimer's disease. Nat Med. 2014;20:1254–62.
39. Zhang Z, Song M, Liu X, Su Kang S, Duong DM, Seyfried NT, et al. Delta-secretase cleaves amyloid precursor protein and regulates the pathogenesis in Alzheimer's disease. Nat Commun. 2015;6:8762.
40. Sterneck E, Tessarollo L, Johnson PF. An essential role for C/EBPbeta in female reproduction. Genes Dev. 1997;11:2153–62.
41. Xu M, Zhang DF, Luo R, Wu Y, Zhou H, Kong LL, et al. A systematic integrated analysis of brain expression profiles reveals YAP1 and other prioritized hub genes as important upstream regulators in Alzheimer's disease. Alzheimers Dement. 2018;14:215–29.
42. Huang Y, Mahley RW. Apolipoprotein E: structure and function in lipid metabolism, neurobiology, and Alzheimer's diseases. Neurobiol Dis. 2014;72 Pt A:3–12.
43. Strohmeyer R, Shelton J, Lougheed C, Breitkopf T. CCAAT-enhancer binding protein-beta expression and elevation in Alzheimer's disease and microglial cell cultures. PloS ONE. 2014;9:e86617.
44. Tanaka T, Akira S, Yoshida K, Umemoto M, Yoneda Y, Shirafuji N, et al. Targeted disruption of the NF-IL6 gene discloses its essential role in bacteria killing and tumor cytotoxicity by macrophages. Cell. 1995;80:353–61.
45. Verghese PB, Castellano JM, Holtzman DM. Apolipoprotein E in Alzheimer's disease and other neurological disorders. Lancet Neurol. 2011;10:241–52.
46. Akiyama H, Barger S, Barnum S, Bradt B, Bauer J, Cole GM, et al. Inflammation and Alzheimer's disease. Neurobiol Aging. 2000;21:383–421.
47. Finch CE, Morgan TE. Systemic inflammation, infection, ApoE alleles, and Alzheimer disease: a position paper. Curr Alzheimer Res. 2007;4:185–9.
48. Theendakara V, Peters-Libeu CA, Bredesen DE, Rao RV. Transcriptional effects of ApoE4: relevance to Alzheimer's disease. Mol Neurobiol. 2018;55:5243–54.
49. Theendakara V, Patent A, Peters Libeu CA, Philpot B, Flores S, Descamps O, et al. Neuroprotective Sirtuin ratio reversed by ApoE4. Proc Natl Acad Sci U S A. 2013;110:18303–8.
50. Lattanzio F, Carboni L, Carretta D, Rimondini R, Candeletti S, Romualdi P. Human apolipoprotein E4 modulates the expression of Pin1, Sirtuin 1, and Presenilin 1 in brain regions of targeted replacement apoE mice. Neuroscience. 2014;256:360–9.
51. Yamada T, Kondo A, Takamatsu J, Tateishi J, Goto I. Apolipoprotein E mRNA in the brains of patients with Alzheimer's disease. J Neurol Sci. 1995;129:56–61.
52. Yamagata K, Urakami K, Ikeda K, Ji Y, Adachi Y, Arai H, et al. High expression of apolipoprotein E mRNA in the brains with sporadic Alzheimer's disease. Dement Geriatr Cogn Disord. 2001;12:57–62.
53. Zarow C, Victoroff J. Increased apolipoprotein E mRNA in the hippocampus in Alzheimer disease and in rats after entorhinal cortex lesioning. Exp Neurol. 1998;149:79–86.
54. Diedrich JF, Minnigan H, Carp RI, Whitaker JN, Race R, Frey W 2nd, et al. Neuropathological changes in scrapie and Alzheimer's disease are associated with increased expression of apolipoprotein E and cathepsin D in astrocytes. J Virol. 1991;65:4759–68.
55. Shao Y, Gearing M, Mirra SS. Astrocyte-apolipoprotein E associations in senile plaques in Alzheimer disease and vascular lesions: a regional immunohistochemical study. J Neuropathol Exp Neurol. 1997;56:376–81.
56. Martins RN, Taddei K, Kendall C, Evin G, Bates KA, Harvey AR. Altered expression of apolipoprotein E, amyloid precursor protein and presenilin-1 is associated with chronic reactive gliosis in rat cortical tissue. Neuroscience. 2001;106:557–69.
57. Hesse C, Larsson H, Fredman P, Minthon L, Andreasen N, Davidsson P, et al. Measurement of apolipoprotein E (apoE) in cerebrospinal fluid. Neurochem Res. 2000;25:511–7.
58. Gupta VB, Laws SM, Villemagne VL, Ames D, Bush AI, Ellis KA, et al. Plasma apolipoprotein E and Alzheimer disease risk: the AIBL study of aging. Neurology. 2011;76:1091–8.

59. Cramer PE, Cirrito JR, Wesson DW, Lee CY, Karlo JC, Zinn AE, et al. ApoE-directed therapeutics rapidly clear beta-amyloid and reverse deficits in AD mouse models. Science. 2012;335:1503–6.
60. Kfoury N, Kapatos G. Identification of neuronal target genes for CCAAT/enhancer binding proteins. Mol Cell Neurosci. 2009;40:313–27.
61. Xia J, Hu B, Mu Y, Xin L, Yang S, Li K. Molecular cloning and characterization of the promoter region of the porcine apolipoprotein E gene. Mol Biol Rep. 2014;41:3211–7.
62. Sen A, Nelson TJ, Alkon DL. ApoE4 and Abeta oligomers reduce BDNF expression via HDAC nuclear translocation. J Neurosci. 2015;35:7538–51.